NASA Contractor Report 159121

Application of Tunable Diode Lasers as Local Oscillators in an Infrared Heterodyne Radiometer [IHR]

M.G. Savage, R.C. Augeri, and B.J. Peyton

Eaton Corporation
AIL Division
Melville, N. Y. 11747

CONTRACT NAS1-14362
DECEMBER 1979

National Aeronautics and
Space Administration

Langley Research Center
Hampton, Virginia 23665

NASA Contractor Report 159121

Application of Tunable Diode Lasers as Local Oscillators in an Infrared Heterodyne Radiometer [IHR]

M.G. Savage, R.C. Augeri, and B.J. Peyton

Eaton Corporation
AIL Division
Melville, N. Y. 11747

CONTRACT NAS1-14362
DECEMBER 1979

National Aeronautics and
Space Administration

Langley Research Center
Hampton, Virginia 23665

TABLE OF CONTENTS

I. INTRODUCTION

Recent developments in the area of tunable semiconductor diode lasers (TDLs) have stimulated interest in their potential application to heterodyne spectroscopy. Heretofore, the outputs of TDLs have been characterized by low CW powers, regions of multiple wavelength modes, and non-Gaussian intensity distributions which have rendered them unsuitable for most coherent applications. Currently available diode lasers have overcome some of these previous limitations. This program was aimed at evaluating the present state of the semiconductor laser technology with respect to utilization of TDLs as local oscillators in an infrared heterodyne spectrometer.

Based on both theoretical considerations and experimental data, detailed TDL specifications were developed and used to purchase two current state-of-the-art TDL devices. The TDL specifications which were generated are not optimum with respect to heterodyne application but represent a compromise between what is currently achievable and what is desired for good heterodyne receiver performance. In most cases each of the performance specifications have been previously surpassed in selected TDL devices. However, the specifications represent a complete characterization of the TDL since they require that all of the performance characteristics objectives be achieved simultaneously.

A detailed test program has been carried out to determine the utility of the diode lasers as local oscillators (LOs) in a heterodyne receiver application. The program included measurements

of the CW power, spectral tunability, spectral stability, and spatial intensity distribution of the TDL outputs. A tunable diode laser LO was incorporated into a laboratory Dicke-switched infrared heterodyne setup and used to measure radiometer sensitivity as well as spectroscopic characteristics of selected absorption lines of ammonia. This report emphasizes the test results on one (TDL-A5) of the two tunable diode lasers in an attempt to provide a comprehensive data package which may be useful for future planning purposes. The second tunable diode laser (TDL-A6) exhibits characteristics similar to the fully tested TDL with the exception that some changes in its performance characteristics as it was temperature cycled between room temperature and the operating temperature of approximately 50K occurred.

As a result of this TDL test program some initial conclusions have been reached as to the current state of semiconductor laser technology and their suitability as LO sources in heterodyne spectrometers. Some suggestions in the areas of future laser development and TDL utilization are presented in Section V.

II. TEST SETUP FOR TDL EVALUATION

Laboratory measurement of a tunable diode laser local oscillator (LO) in a passive infrared heterodyne receiver test setup is one of the principal objectives of this program. In particular, the program is aimed at providing TDL measurement data for the design of an engineering model of a tunable infrared heterodyne radiometer which can measure atmospheric pollutants from airborne platforms.

A detailed TDL specification was generated and used to obtain two tunable lead-salt alloy diode lasers for test and evaluation. The devices, which were purchased from Laser Analytics, Inc., Lexington, Ma, were mounted in the vacuum section of a CTI Model 21 refrigerator. This refrigerator is capable of maintaining the temperature of the lasers at any desired value between 12K and 300K with a nominal temperature stability of $\pm$ 0.003K over a 50-minute time period. A regulated-current power supply which is capable of delivering up to two amperes of dc current is used to energize the diode lasers. The noise plus ripple content of the power supply output current is nominally $\pm$ 15 microamperes.

The diode lasers, cooler, cables, and current driver were integrated into a versatile laboratory test setup (Figure 2-1) which included:

- A wideband PV:HgCdTe detector for both the heterodyne and direct detection measurements.
- A narrowband PV:HgCdTe detector for measurement of the available TDL power at the monochromator output.

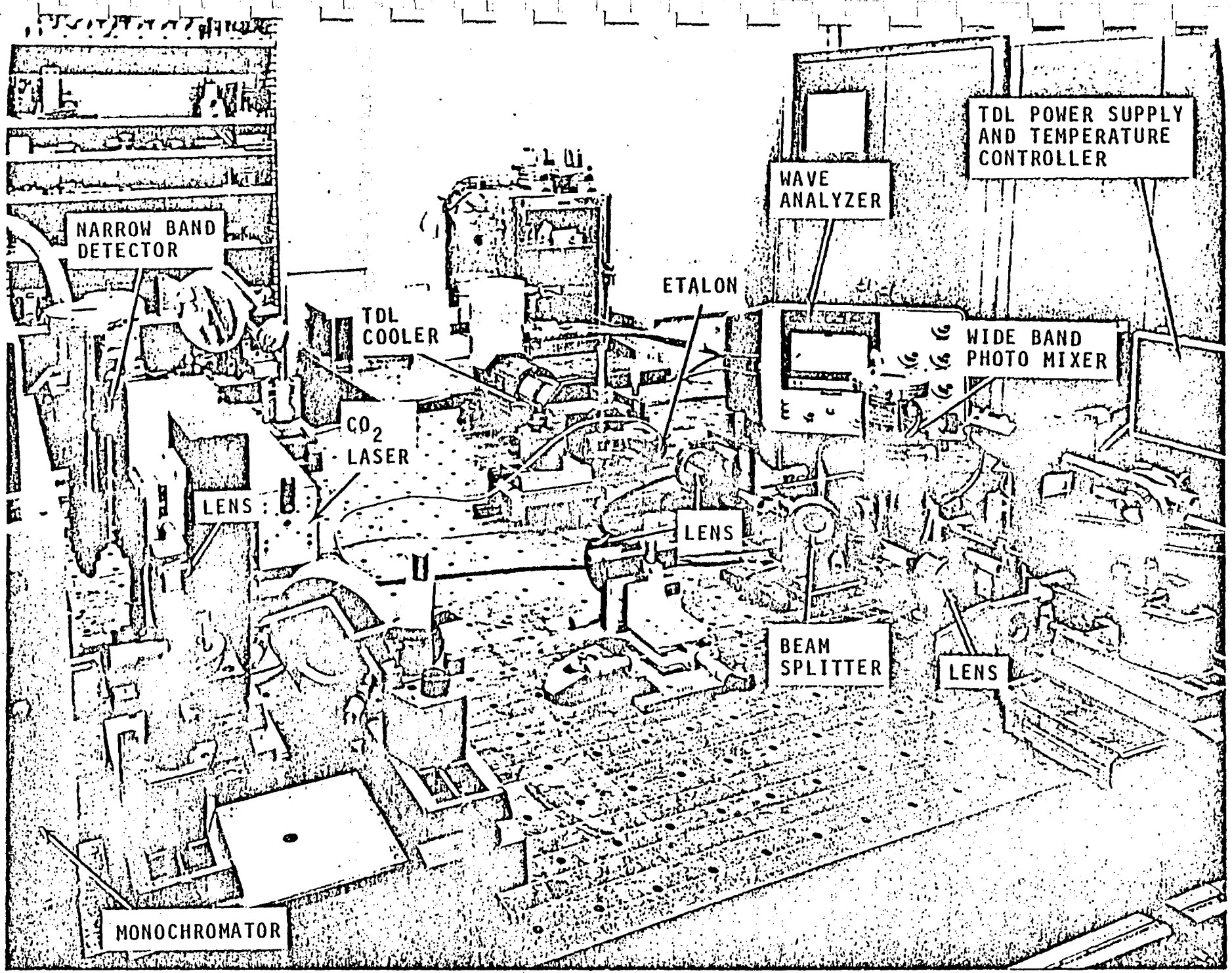

FIGURE 2-1. TDL LABORATORY TEST SETUP

- A Spex monochromator Model No. 1700 for laser wavelength determination.
- An AIL Model 707 spectrum analyzer for the measurement of (1) the TDL-CO_2 laser beat frequencies, and (2) the TDL self-beating effects.
- An AIL Model 2392C radiometric processor for the spectral examination of pollutant absorption lines.
- A Hewlett-Packard Model 3581A wave analyzer for the direct detection measurement of the TDL output power.

The results of the direct detection measurements using TDL-A5 as the signal source are summarized in Section III and the results of the heterodyne measurements using TDL-A5 as a local oscillator source are summarized in Section IV. The test measurements of this program were aimed at evaluating the TDL elements for ultimate utilization in a heterodyne spectrometer. No attempt was made to optimize the heterodyne receiver setup, however a comparison of receiver data which were obtained using either a diode laser or a gas laser LO is a direct performance comparison of the TDL and gas laser. Versatile test setups were employed, wherever possible, in order to expedite the complete characterization of the TDL devices.

III. DIRECT DETECTION MEASUREMENTS OF TUNABLE DIODE LASERS

Detailed direct detection measurements have been carried out to evaluate the tunable diode lasers (TDLs) under laboratory conditions. This section describes measurements of TDL output power, spectral tuning range, spectral tuning rates, spectral modes, and spatial intensity distributions.

The measurement of TDL output power resulted in maximum multimode power levels of approximately 200 μW at an injection current of I_{DC} = 1.62 ampere for TDL-A5 and approximately 175 μW at I_{DC} = 1.69 ampere for TDL-A6. Maximum single-mode powers were approximately 125 μW for TDL-A5 and 100 μW for TDL-A6. The measured spectral mode separation of both TDLs was approximately two wavenumbers.

It should be noted that these output powers are available in highly divergent beams which must be captured and collimated for local oscillator applications. The amount of single-mode TDL LO power available at the photomixer of a heterodyne spectrometer is expected to be typically 20 to 80 μW. This available power depends on (1) the injection current and junction temperature (which fix the emission wavelength), (2) the beam divergence and its requisite optics, and (3) the signal/local oscillator combining technique.

A simplified diagram of the test setup used to measure the TDL threshold current, output power and spectral tuning characteristics is given in Figure 3-1. The divergent power output of the TDL is collimated by 5 cm f/1 germanium miniscus lens configured for minimum spherical aberration. (All of the refractive optics

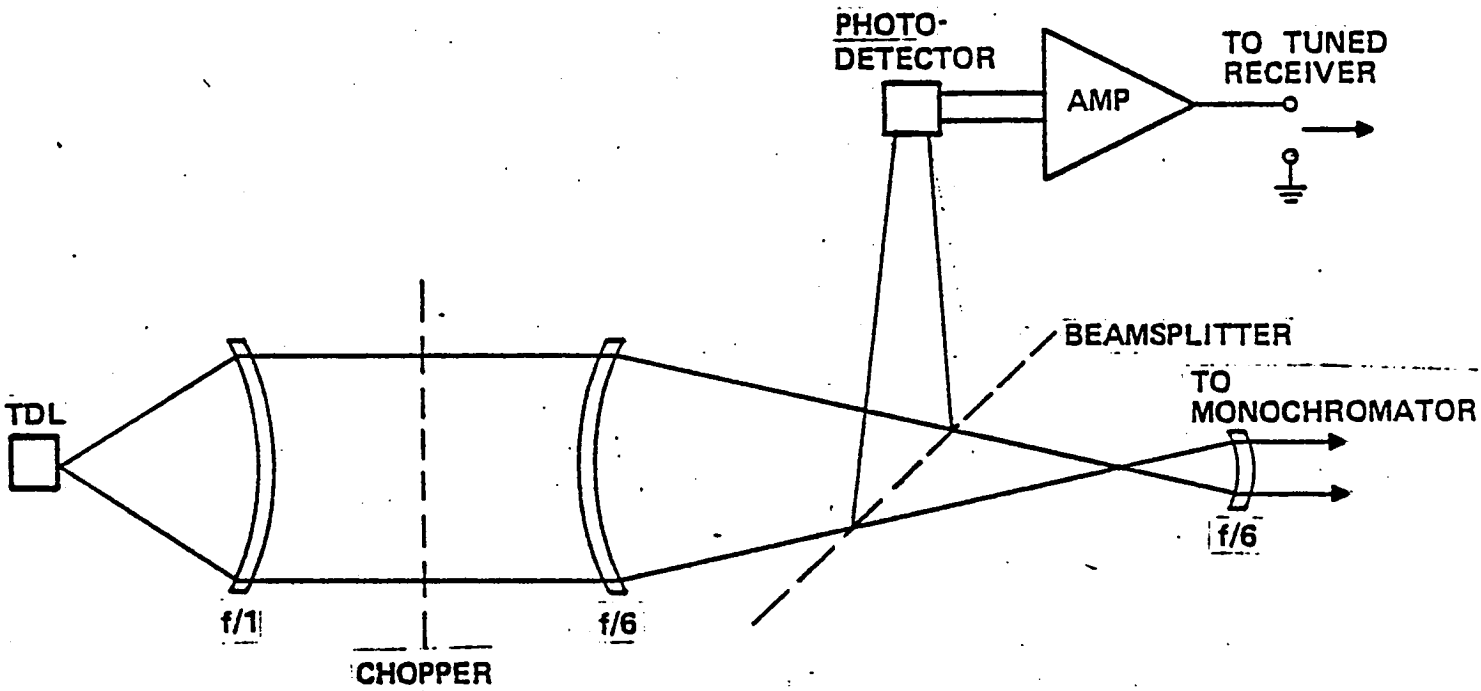

Figure 3-1. Test Setup for Measurement of the Emission Wavelengths and Threshold Currents of TDL's.

used for the tests were germanium miniscus lenses which were AR-coated for operation near λ = 10 μm and configured for minimum spherical aberration.) The collimated beam is chopped and focused by a 5 cm f/6 lens. Seventy percent of the TDL power is directed by a beam splitter onto a wideband PV:HgCdTe detector whose output is amplified and fed to a receiver (wave analyzer) which is tuned to the chopping frequency.

A. Lasing Thresholds

For a semiconductor laser the condition for optical gain can be expressed as (Ref. 1):

$$\left| \psi_n - \psi_p \right| \geq hc/\lambda \qquad (3\text{-}1)$$

where ψ_n and ψ_p are the quasi-Fermi levels of the minority and majority carriers, respectively, and λ is the output wavelength. There is a minimum minority carrier density, n_t, below which the TDL will exhibit no gain. More precisely, n_t is that value of injected minority carrier density needed to satisfy the equality in (3-1). To a certain extent the values of ψ_n and ψ_p are selectable during manufacture by variation of the diode's doping. Through ψ_n and ψ_p, the value of n_t, and hence I_T, is a complicated function of temperature and device geometry.

As the dc current through the TDL is increased the diode laser emits larger amounts of broadband fluorescence-like radiation until the lasing threshold current, I_T, is attained. At the lasing threshold current there is a very rapid increase in the TDL emission intensity as well as a pronounced narrowing of the emission spectrum

(Refs. 1, 2 and 3). Measurement of the lasing threshold current was accomplished by increasing the injected current until an abrupt increase in the TDL output power was observed. The temperature of the diode was then changed and the laser's threshold current was again measured after a two to three minute stabilization period. The measured lasing threshold currents as a function of heat sink temperature are given in Figure 3-2. These measured currents varied from approximately 0.62 ampere at T = 40K to 1.35 amperes at T = 59K.

Because of the high reflectivity of the beam splitter and unavoidable losses throughout the optical train, several microwatts of emitted TDL power were required to make an accurate wavelength measurement. For injection currents which are just above the threshold level the emitted TDL power increases very rapidly with increasing current, therefore the measured TDL emission wavelength at a current which is slightly larger (0.1 amp) than the threshold setting is expected to be fairly representative of the emission wavelength at threshold. The measured wavelength at threshold as a function of the heat sink temperature is given in Figure 3-3. As can be seen, the TDL emission wavelength at threshold varied between approximately 938 cm^{-1} ($\lambda \approx 10.6$ μm) at T = 59.5K and 862 cm^{-1} ($\lambda \approx 11.6$ μm) at T = 39K.

Based on theoretical considerations, several investigators have predicted the relationship between the laser threshold current density and the laser temperature (Refs. 1, 2 and 4). The Lasher and Stern Model (Ref. 5) for gallium arsenide devices is also

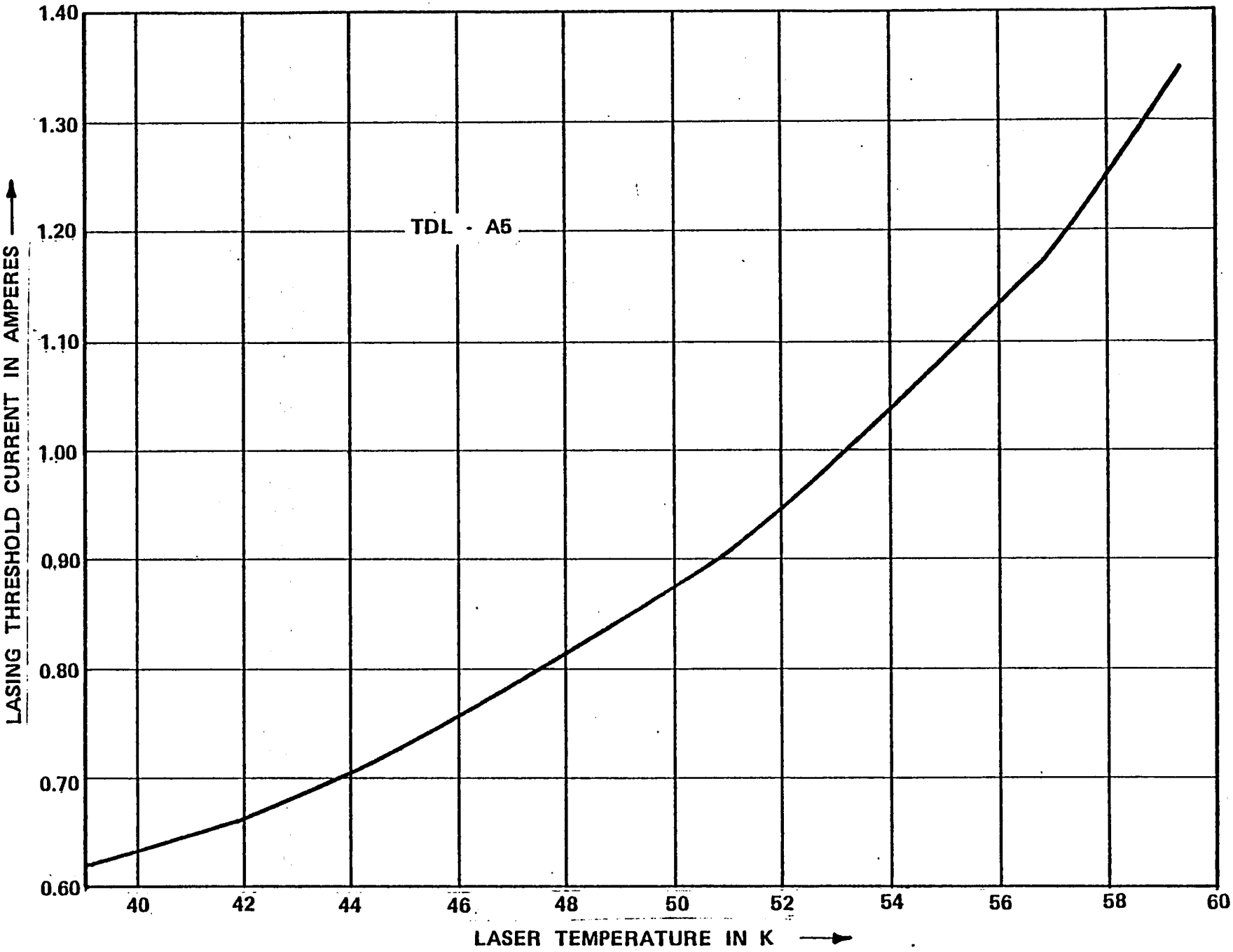

Figure 3-2. Measured Lasing Threshold Current vs. Laser Temperature.

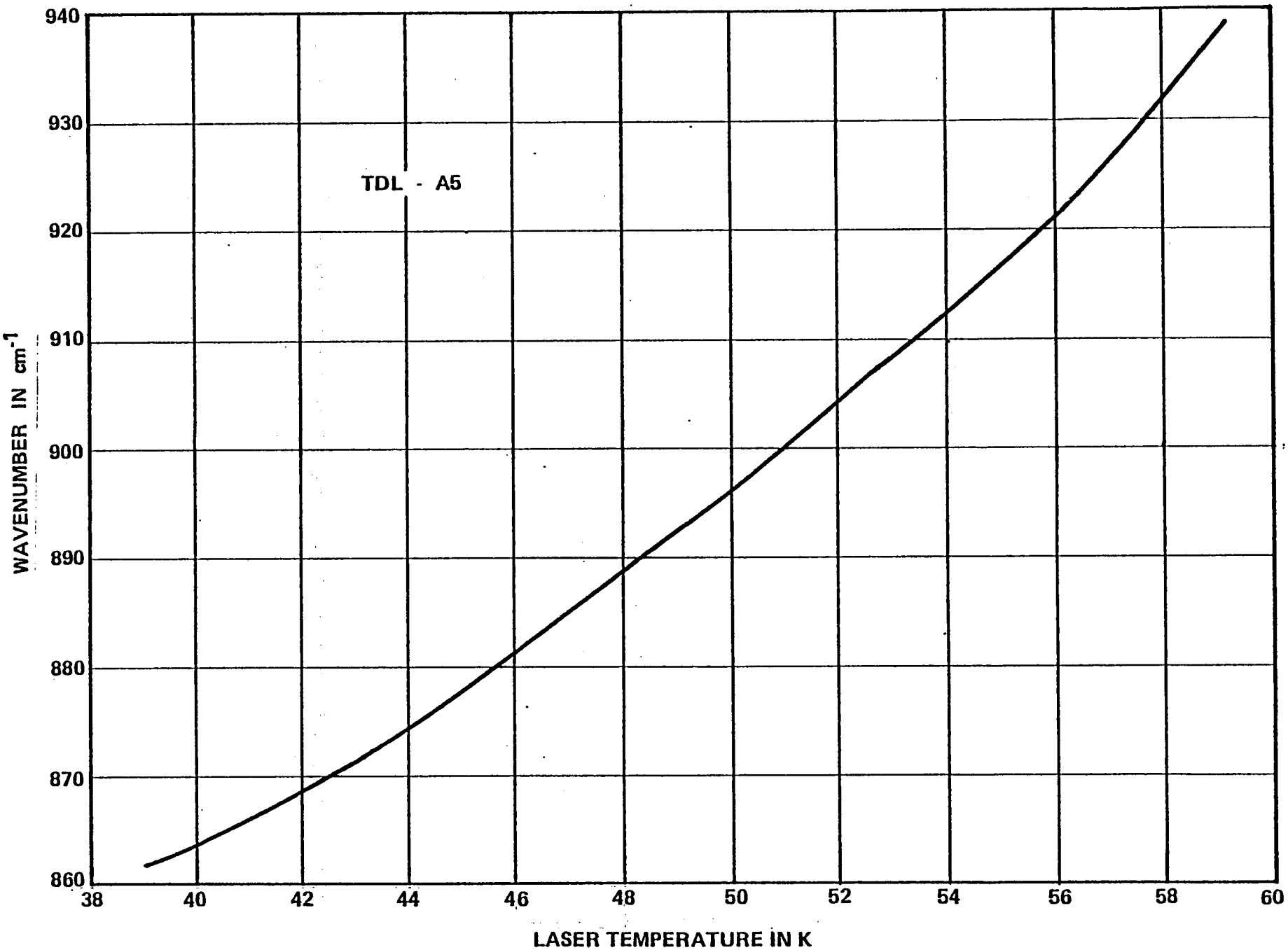

Figure 3-3. Measured TDL Emission Wavelength at Threshold vs. Laser Temperature.

believed to be representative of single heterostructure lead-salt alloy devices. The data shown in Figure 3-2 are consistent with the predicted behavior (Ref. 4). More detailed information on the stoichiometry and construction of the diode lasers as well as additional measured data is required for precise verification of these models.

B. TDL Tunability and Tuning Rates

The minimum energy gap, E_g, determines the TDL emission wavelength. The emission wavelength is given (Ref. 4) by:

$$\lambda = \frac{1.24}{E_g} \qquad (3\text{-}2)$$

where E_g is given in electron-volts and λ is given in micrometers. For an emission wavelength of λ = 10.78 μm (927.6 cm^{-1}), E_g is of the order of 0.12 eV. Previous investigators (Refs. 4 and 6) have determined that E_g ranges from 0.19 eV to 0 eV in $Pb_{1-x}Sn_xTe$ when x ranges from 0 to 0.35; this corresponds to TDL emission wavelengths in the range of approximately 6.5 μm to 30 μm.

Thermal considerations are acknowledged to be responsible for the tunability of semiconductor lasers due to the variation of the energy gap with junction temperature (Ref. 4). Current tuning is actually a manifestation of junction temperature tuning. The TDL spectral tuning rate, $\Delta\nu/\Delta I$, is due to the joule heating of the junction caused by the injected current I_{DC} and is fixed primarily by the thermal resistance between the junction and the refrigerator's heat sink. Lead-salt alloys typically exhibit high

thermal resistances which can be of the order of 0.01 W/cm-K (Ref. 4). Such high thermal resistance has allowed other investigators (Ref. 4) to measure junction temperatures in the neighborhood of 40K for heat sink temperatures near 7K. The thermal conductivity is a parameter which is determined by the stoichiometry of the TDL alloy. The change of TDL frequency with injection current is also somewhat adjustable by variation of the diode-heat sink geometry (Ref. 7).

The TDL emission wavelength was measured as a function of injected dc current for refrigerator heat sink temperatures of 50.23K and 57.6K: the results are given in Figures 3-4 and 3-5. The data in Figures 3-4, 3-5, and 3-6 demonstrate the TDL emission wavelength's dependence on both junction temperature and injection current. The solid points in Figure 3-4 were measured with a monotonically increasing injection current while the open-circle points at 1.275 amperes were measured with the current monotonically decreasing. These open-circle points displace the corresponding solid circle points at 898.25 cm^{-1}. From these results it is apparent that the manner in which the injection current is varied is important to the determination of the maximum single-mode tuning range. It should be noted that the slopes of the wavelength-current tuning curves varied between 90 MHz/mA and 135 MHz/mA. The wavelength-temperature tuning rate for TDL-A5 was approximately 16 GHz/K.

In principle, once threshold has been achieved, a diode laser tuned solely by variation of its heat sink temperature is identical to a laser which is tuned by variation of its injected current. In practice, however, I_{DC} is usually more readily and more accurately adjustable. Comparison of Figure 3-4 and Figure 3-6 illustrates the equivalence of temperature and injection current.

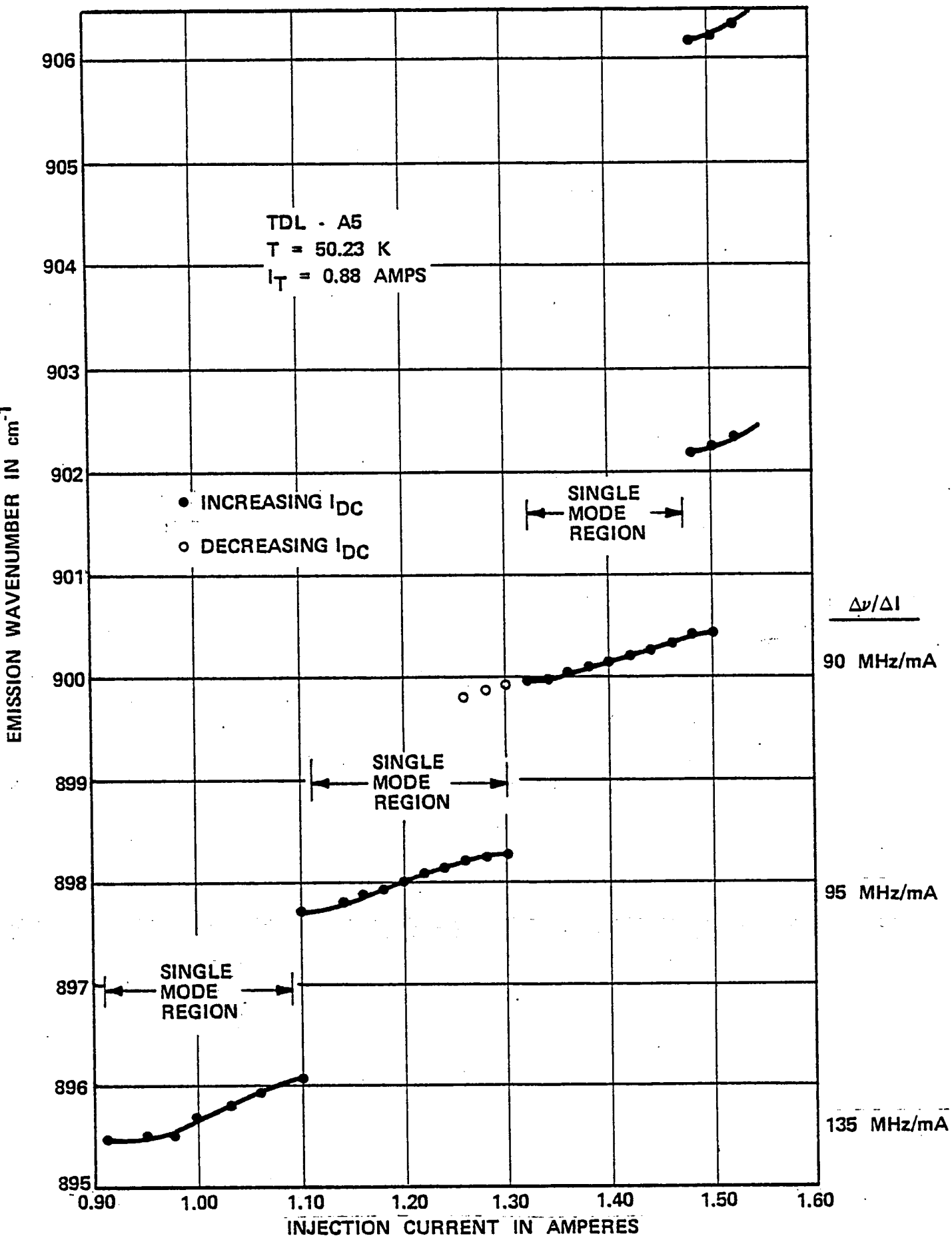

Figure 3-4. Measured TDL Emission Wavelength vs. Injection Current for T = 50.23 K

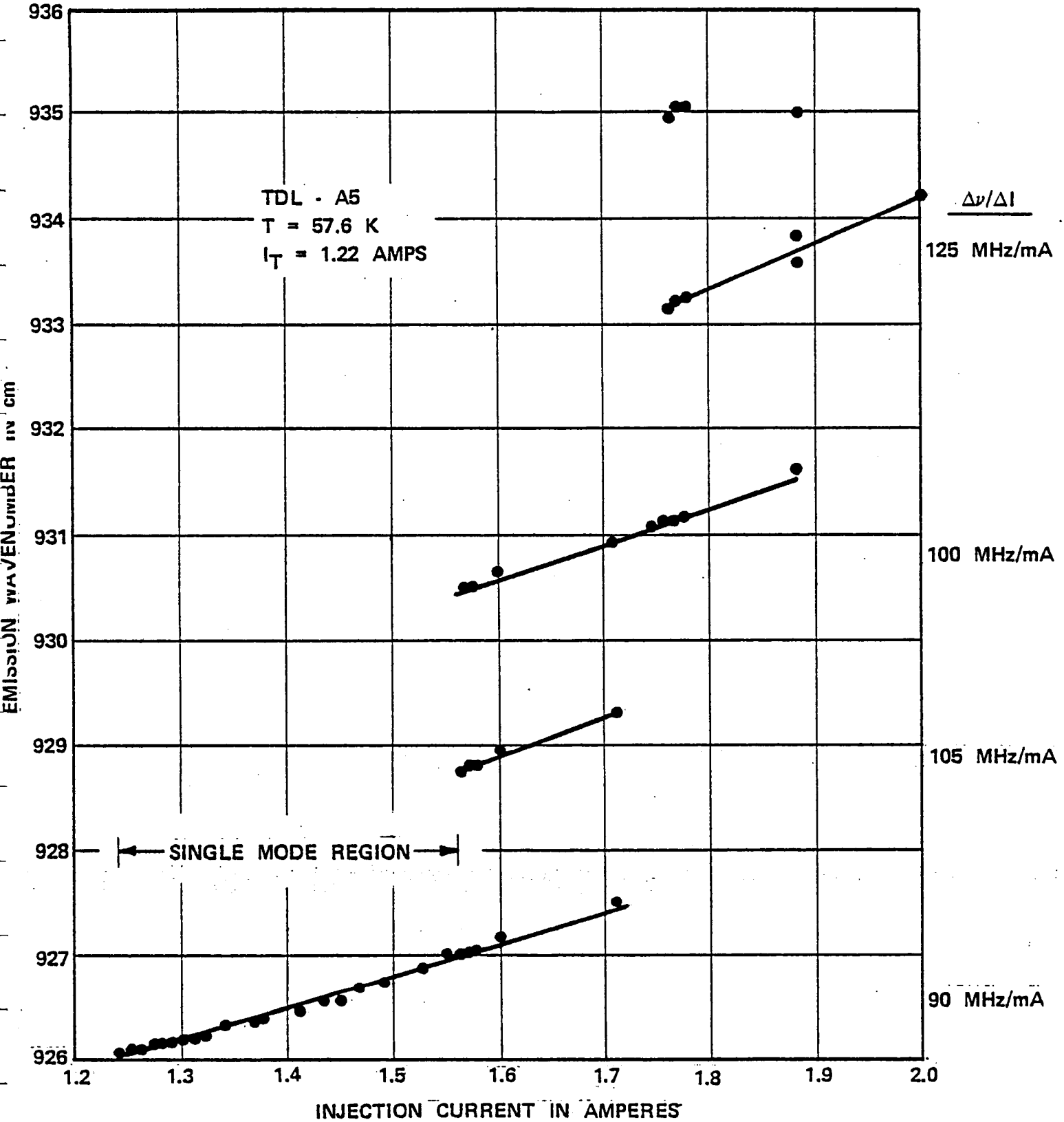

Figure 3-5. Measured TDL Emission Wavelength vs. Injection Current for T = 57.6 K.

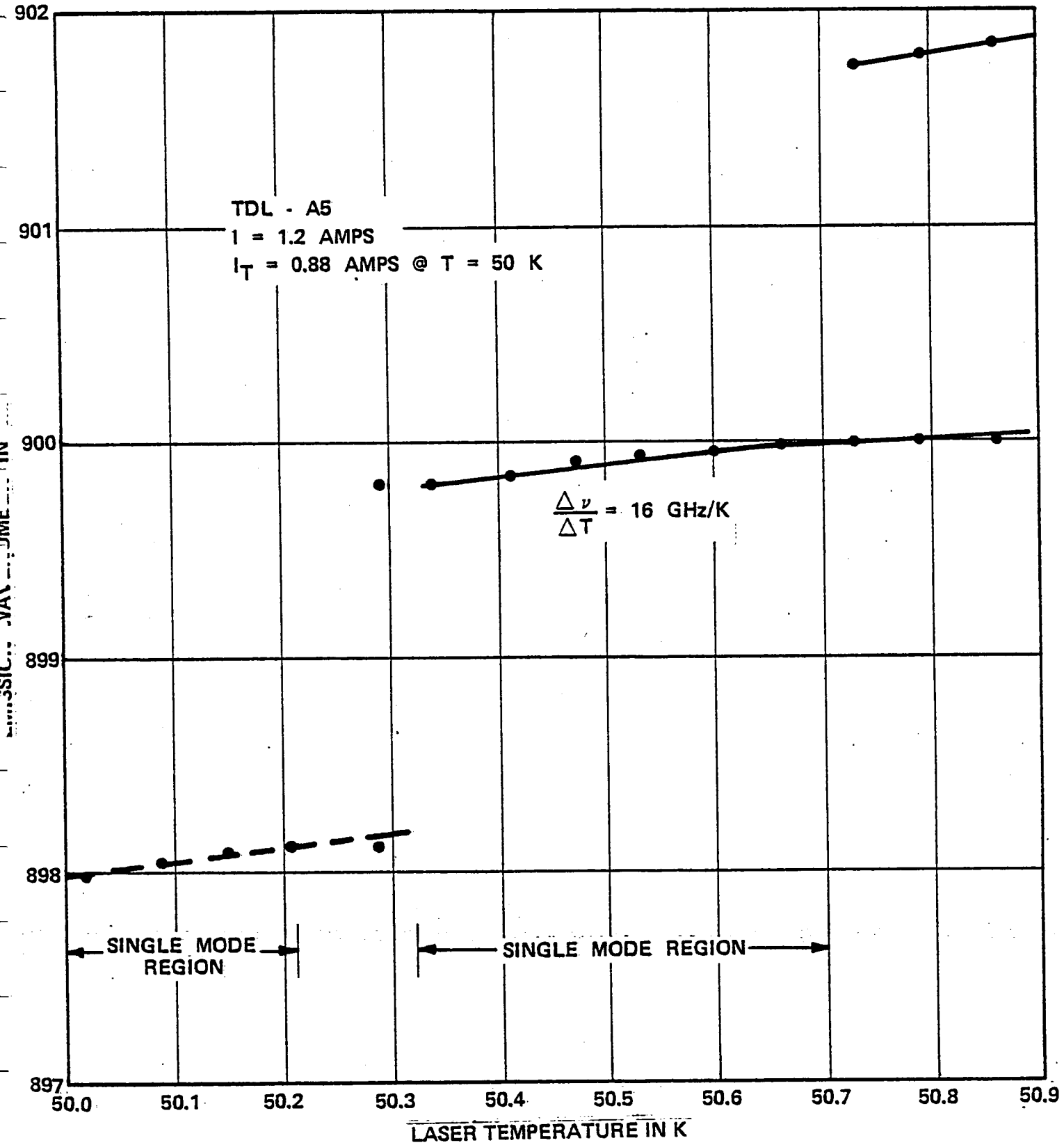

Figure 3-6. Measured TDL Emission Wavelength vs. Cooler Terminal Temperature for an Injection Current of 1.2 Amperes.

Based on the measured data in Figure 3-5, the positioning of the temperature so that a cavity mode exists for a value of I_{DC} approximately equal to the threshold value appears to extend the single-mode tuning range of the laser. The spectral mode in Figure 3-5 at 926.5 cm^{-1} had a tuning range of approximately $\pm$ 0.5 cm^{-1} while some of the other modes, shown in Figures 3-4 and 3-5, which did not exist near threshold were tunable over a narrower $\pm$ 0.3 cm^{-1} range. It has not yet been determined whether this phenomenon occurs for any mode in coincidence with the threshold current.

From Figures 3-4 and 3-5 it can be observed that the diode lasers are piecewise-continuously tunable with the spectral separation between modes, $\Delta\lambda$, of the order of 1.8 cm^{-1}. This spectral spacing between modes is governed by the relation (Ref. 4):

$$\Delta\lambda = \lambda^2/2\ L\ n_D \qquad (3\text{-}3)$$

where L is the cavity length and n_D is the dispersive value of the refractive index of the lasing material. For a nominal TDL cavity length of 300 μm the calculated value of n_D is approximately 8.8 which is slightly greater than previously reported values (Refs. 4, 6, 8 and 9). From equation (3-3) it can be seen that a longer TDL cavity will support spectral modes which are closer together.

It is clear that more than one laser may be required for spectroscopic applications in which a particular 1 cm^{-1} (30 GHz) wavelength region must be completely covered.

C. TDL Radiation Field Patterns

In a diode laser the minority carriers are injected perpendicular to the TDL junction. The current distribution across the

junction is asymmetric to the spatial distribution of the optical gain. As a result the gain for higher order spatial modes may be larger than that for the lowest order mode with the magnitude of the difference being related to the thickness of the TDL junction. Since the diffraction losses for the higher order modes are larger than the diffraction loss for the lowest order, the threshold currents necessary for oscillation in these modes are also larger (Ref. 4).

The output intensity of a diode laser generally exhibits a complex non-Gaussian spatial distribution. For most efficient coupling of the available TDL power onto the photodetector of a spectrometer system, it is felicitous to have some knowledge of this spatial distribution. In the test setup illustrated in Figure 3-7 the position of the photodetector was manually varied in two mutually orthogonal and one diagonal direction. The spatial scans were perpendicular to the optical axis and measurements have been carried out for two values of TDL injection current. For the lower current value the TDL emitted a single wavelength while for the higher current value the laser emitted several wavelengths.

The far field spatial distribution as modified by the lens system (Fourier transform) of the TDL output intensity in a single mode tuning region ($T = 57.5K$, $I = 1.69$ ampere, and $\nu = 930.74\ cm^{-1}$) is given in Figure 3-8. The lens system (Figure 3-7) used for the spatial intensity pattern measurements provided a magnification of twenty to facilitate inspection of the TDL beam.

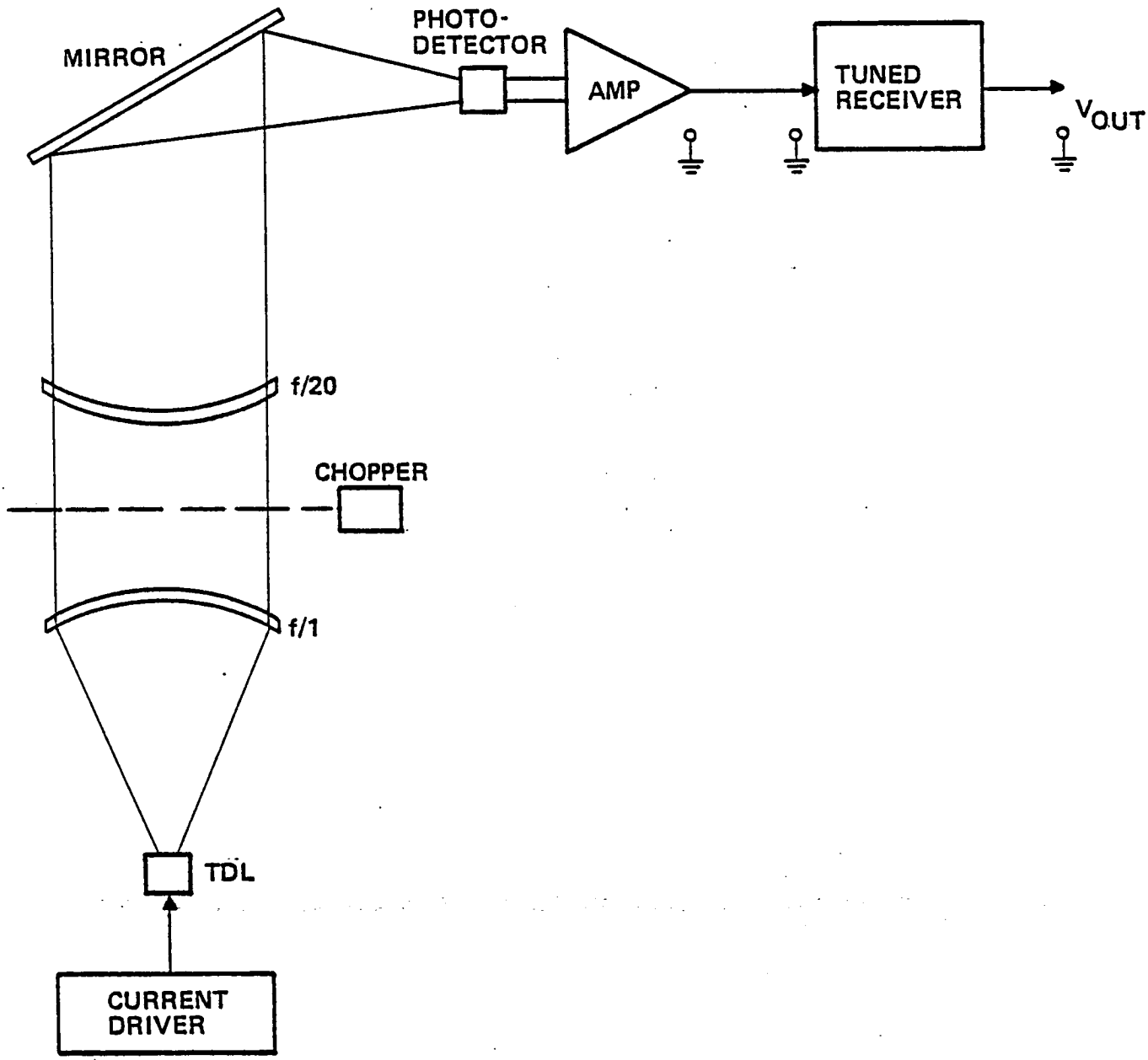

Figure 3-7. Test Setup for Measurement of TDL Spatial Intensity Patterns.

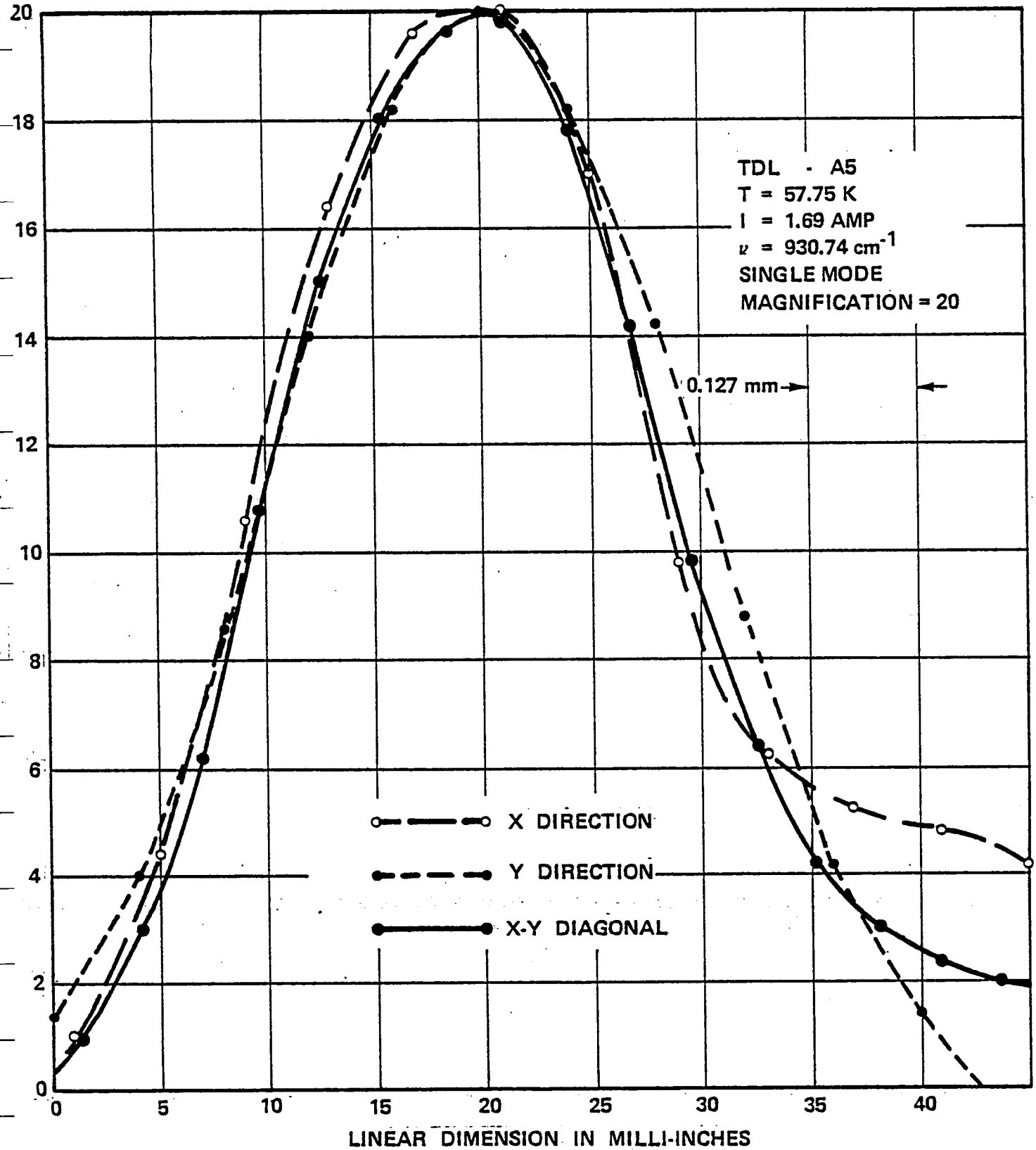

Figure 3-8. Measured Spatial Distribution of the TDL Output Intensity in a Single Mode Region.

It is not possible to measure the spatial pattern of the TDLs without the interfering etalon effects caused by the window of the dewar. However it should be noted that the measured far field spatial distribution through the lens system is believed to be representative of how TDL LOs will be employed in operational heterodyne receivers.

The measured data indicate that the far field distributions of the laser intensities are similarly uniform for the X-, Y-, and X-Y directions except for the slower roll-off on one side of the X-direction* spatial scan. In addition the measured beam pattern was slightly wider in the Y-direction. It is estimated that greater than 40 percent of the output TDL power is available at the focus of the lens system (see Figure 3-7). The measured peak TDL power at the photodetector (Figure 3-7) was approximately 20 μW.

The measured spatial distribution of the TDL output intensity in a multi-mode tuning region (T = 57.75K and I = 1.89 ampere) is given in Figure 3-9. As can be seen, there appears to be power available in two distinct spatial regions. The measured peak power of the principal mode was approximately 30 μW at the photodetector. The shapes of the measured laser intensity are similar for the X-, Y-, and X-Y diagonal directions although the weaker TDL mode was most prominent in the Y-direction.

The X-direction of the measured radiation field patterns of TDL-A5 (shown in Figures 3-8 and 3-9) is perpendicular to the junction and parallel to the injected current vector I. From the apparent asymmetry of the measured TDL spatial pattern in the X-direction

*X-direction is perpendicular to the junction.

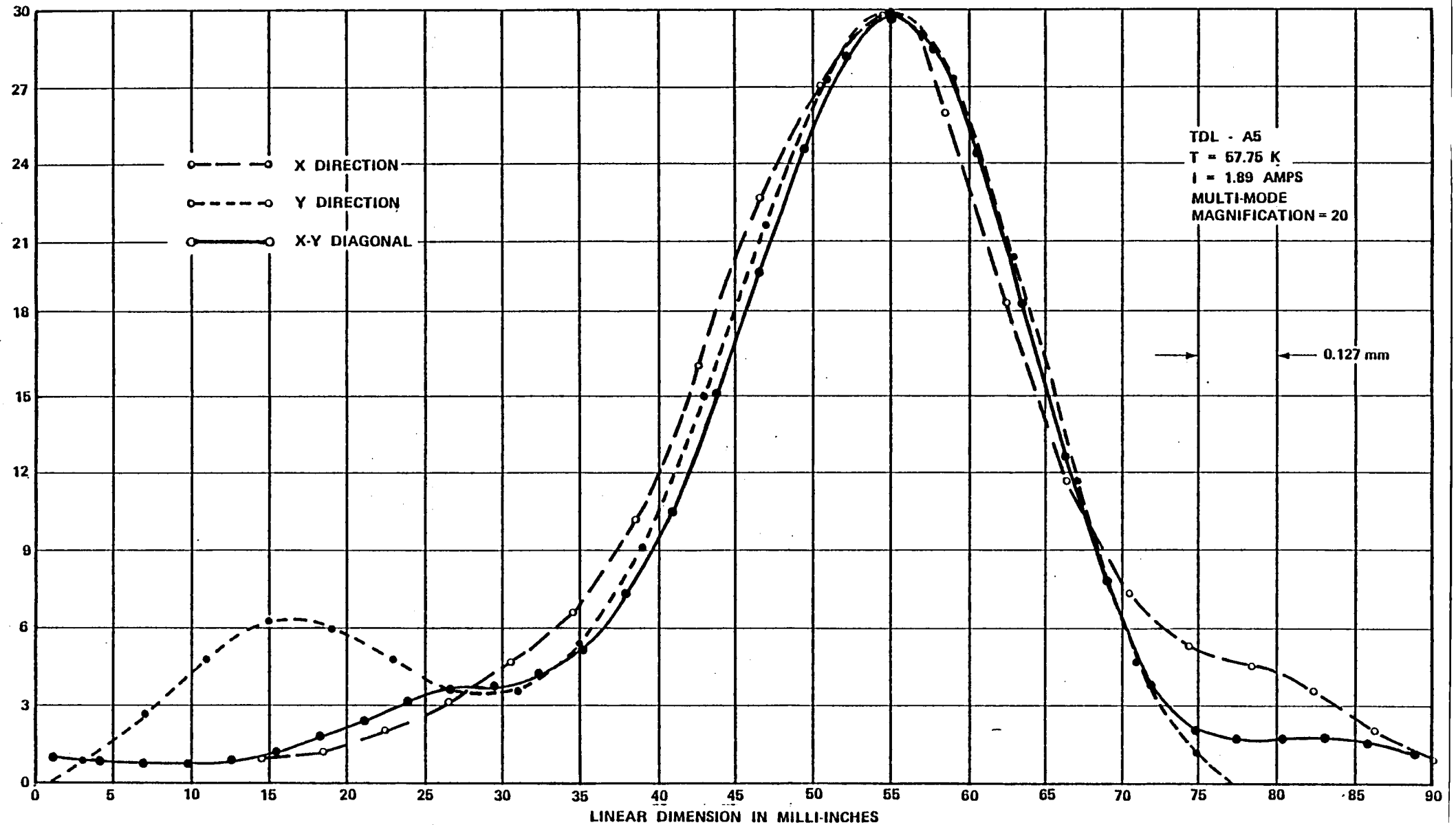

Figure 3-9. Measured Spatial Distribution of the TDL Output Intensity in a Multi-Mode Region.

it can be inferred that the current I_{DC} flows from left to right. It has also been determined that the electric field vector, $\vec{E}$, was polarized parallel to the junction (i.e., along the Y-direction) for TDL-A5. (The E-field vector was oriented at an angle of 45° to the junction for TDL-A6.)

It can be readily observed that the TDL radiation patterns were slightly non-uniform in the wings of both the X- and Y-directions. The measured TDL half-power spatial widths were 0.50 mm (20 milli-inches) and 0.57 mm (22.5 milli-inches) in the perpendicular and parallel directions, respectively. Since the optical setup (see Figure 3-7) has a nominal magnification of 20, the true dimensions of the TDL lasing region are approximately 25 μm by 28.5 μm. The 25 μm dimension agrees with the nominal stripe width (nominally 25 μm to 50 μm) while the 28.5 μm dimension is believed to be related to the width of the uniform current density region in the active TDL junction.

As discussed previously, the injection current must be increased to a value which is greater than the threshold level for higher order mode propagation. The TDL was emitting more than one wavelength when the multi-mode spatial profile data (Figure 3-9) was obtained. The radiation pattern in the perpendicular (X) direction was reasonably uniform and was more nearly centered due to a spatial shift of approximately 8 μm. On the other hand the pattern in the parallel direction (Y) had a pronounced two-lobe structure and was shifted approximately 3 μm. While the laser could have been emitting two wavelengths uniformly in a higher order spatial mode, it is believed likely that each individual wavelength was emitted in a separate parallel-direction lobe (Ref. 4).

The face of the diode laser cavity was formed by a cleavage of the material with the resultant surface left unpolished. The imperfections which result from such face formulation produce several potential optical cavities of slightly differing lengths which may support oscillation either singly or multiply. Filamentary lasing of this nature has been discussed by several investigators (Refs. 1, 4 and 6). Based on device geometry considerations, the spatial width of the injected current measured along the junction (i.e., along the Y-direction) is expected to increase as the TDL current increases. The local current density in the various cavities formed by the surface imperfections may eventually exceed the individual threshold values for these cavities. Under these conditions the TDL output will be composed of several closely-spaced simultaneously-emitted wavelengths (see Figure 3-5 at I_{DC} = 1.88 amps). In Figure 3-5, the simultaneously-emitted wavelengths are separated by 1.5 to 2 cm^{-1} and are the lowest order eigenmodes of the resonator determined by the nominal dimensions of the TDL device. The two points located between 933.5 cm^{-1} and 934 cm^{-1} are too close together to be such eigenmodes but appear to be consistent with a filamentary lasing explanation (Ref. 4). As the TDL injected current was further increased, higher order eigenmodes of the resonator were excited. These high order modes were revealed by a wavelength-band output of the diode. These bands, as measured by the monochromator, were approximately 0.3 cm^{-1} in width and were separated by the nominal mode spacing of 1.5 to 2 cm^{-1}.

Multiple wavelength TDL outputs will have seriously detrimental effects on heterodyne spectrometer systems using these TDLs as LOs since such uncorrected outputs reduce the attainable spectral resolution. In addition, receiving systems that employ high resolution tunable Fabry-Perot Etalons (FPEs) either as LO filters or LO frequency calibrators mayalso experience problems with multi-mode TDLs.

D. Compatibility of TDL and Fabry-Perot Etalon

In a remotely operated infrared heterodyne spectrometer a wavelength calibration technique is required when the laser is tuned over several wavelength modes. Several passive calibration methods have been considered which involve the use of rotatable gratings or tunable FPEs. In general the use of grating and etalon devices requires well-collimated TDL radiation in order to achieve maximum efficiency in wavelength selectivity.

A series of laboratory measurements was performed to determine the compatibility of the tunable diode lasers and a FPE. A 1.25 cm diameter tunable etalon with a finesse of F = 25 was inserted into the nominally collimated TDL beam. Spectral tuning of the etalon passbands while noting the maximum transmitted power, P_{MAX}, and the minimum transmitted power, P_{MIN}, permits the calculation of the contrast ratio, C, and, hence, of the effective finesse, F_{EFF}. The measured value of the effective finesse is an indication of the degrees of collimation and spectral purity of the incident TDL radiation; the measured data is presented in Table 3-1.

Table 3-1. MEASURED EFFECTIVE FABRY-PEROT ETALON FINESSE VS TDL INJECTION CURRENT FOR TDL-A5, T = 52.95K and I_T = 0.98 A

TDL Current I_{DC} (A)	Max Power P_{MAX} (REL)	Min Power P_{MIN} (REL)	Effective Finesse F_{EFF}
1.0	0.027	0.002	5.55
1.2	0.79	0.019	10.00
1.3	1.14	0.023	10.94
1.35	1.29	0.022	11.92
1.4	1.30	0.023	11.70
1.45	1.29	0.027	10.74
1.5	1.14	0.040	8.23
1.6	1.38	0.043	8.75
1.75	1.24	0.054	7.36
1.8	1.15	0.043	7.97
2.0	1.08	0.120	3.02

In order to achieve its optimum spectral resolution a FPE must be irradiated by collimated radiation. As shown in Figure 3-1, the f/1 lens captures and collimates the TDL emission. For a lens with spherical surfaces perfect collimation can only be achieved if the incident radiation is uniformly emitted from a circular area. Elliptical or linear radiation sources require the use of aspheric or cylindrical lenses. Any degradation in the collimation or monochromaticity (such as TDL multi-mode and fluorescent emission) of the incident radiation will reduce the apparent finesse of the etalon filter. For an etalon with a fixed free spectral range (passband separation) the etalon passbands will widen as the finesse decreases according to the relation:

$$F = \frac{\text{passband separation}}{\text{passband width at half maximum}} \qquad (3\text{-}4)$$

The nominal finesse of the etalon used to collect the data in Table 3-1 was 25. The etalon was adjusted so that its passband width was approximately 500 MHz (0.017 cm^{-1}). Using equation (3-4), the etalon passband separation was approximately 12.5 GHz (0.42 cm^{-1}). As indicated in Figures 3-4, 3-5, and 3-6, the separation between wavelength modes of TDL-A5 is of the order of 1.7 cm^{-1}. Therefore multiple wavelength TDL modes could not be completely rejected by this etalon but would be transmitted to varying extents through separate etalon passbands. The measurements in Table 3-1 are consistent with a multiwavelength explanation. For certain values of injected dc current the laser was operating multi-mode as shown in Figures 3-4 and 3-5. As the etalon, which was placed between the f/1 and f/6 lenses (see Figure 3-1), was spectrally tuned the output

of the photodetector exhibited local maxima corresponding to the spectral overlap of an etalon passband and a TDL emission wavelength. For a single-mode TDL the detector output should show maxima separated by an amount close to the nominal passband separation. In Table 3-1 it can be inferred that this most nearly occurred at an I_{DC} of approximately 1.4 amperes where the measured finesse was then at its maximum. The reduced apparent etalon finesse at this current may be caused by a combination of imperfect collimation and multi-wavelength emission. The further reduction of the apparent etalon finesse is clearly caused by a multi-mode TDL output. A single etalon capable of rejecting the adjacent TDL modes would require a finesse of well over 100. This impractical requirement can be avoided through the appropriate use of two etalons of lower finesse.

E. Direct Detection Spectroscopic Measurements of Selected Absorption Lines

For the direct detection TDL spectroscopy measurements an absorption test cell was filled with varying partial pressures of gaseous ammonia (NH_3) and nitrogen (N_2). The diode laser was tuned to overlap a selected ammonia absorption line located at 930.76 cm^{-1} (Ref. 10). This ammonia signature line is a member of the Q-branch of the antisymmetric a state of the ν_2 fundamental vibration-rotation band; it is designated aQ (3,3) where (3,3) are the (J,K) angular momentum quantum numbers.

Using the direct detection measurement setup shown in Figure 3-10, spectral line shape and line-center transmission measurements of the selected ammonia (NH_3) absorption line have been carried out. The absorption test cell, shown in Figure 3-10, consists of a 10 cm-long aluminum cylinder with a 5 cm diameter evacuable section. The interior of the test cell is teflon-coated and sealed by NaCl windows. The test cell can be filled with a mixture of any desired gases to an accuracy of $\pm$ 1 torr for pressures which are greater than 10 torr or an accuracy of $\pm$ 0.05 torr for pressures less than 10 torr. For the purpose of measuring an absorption line of ammonia the test cell was initially evacuated, filled with a selected NH_3 pressure (typically either 0.5 torr of 0.1 torr), and then filled to a final total pressure using dry nitrogen gas (N_2). The video bandwidth for the direct detection spectroscopic measurements was B_v = 3 Hz. It must be noted that B_v is the bandwidth of receiver electronics and does not include the bandwidth (stability) of the TDL source (see Section IV).

The measured line profiles are given in Figure 3-11 for an ammonia partial pressure of P_{NH_3} = 0.5 torr and a total cell pressure of P_T = 38 and 76 torr. For P_{NH_3} = 0.5 torr and P_T = 38 torr, the measured half width at half maximum, γ, using TDL-A5 was approximately 585 MHz. For P_{NH_3} = 0.5 torr and P_T = 76 torr, the measured γ was approximately 745 MHz. The widths of the spectral absorption lines were obtained using a TDL tuning rate of 110 MHz/mA.

Direct detection measurements of the transmission at line center through the test cell (see Figure 3-10) for P_{NH_3} = 0.5 torr

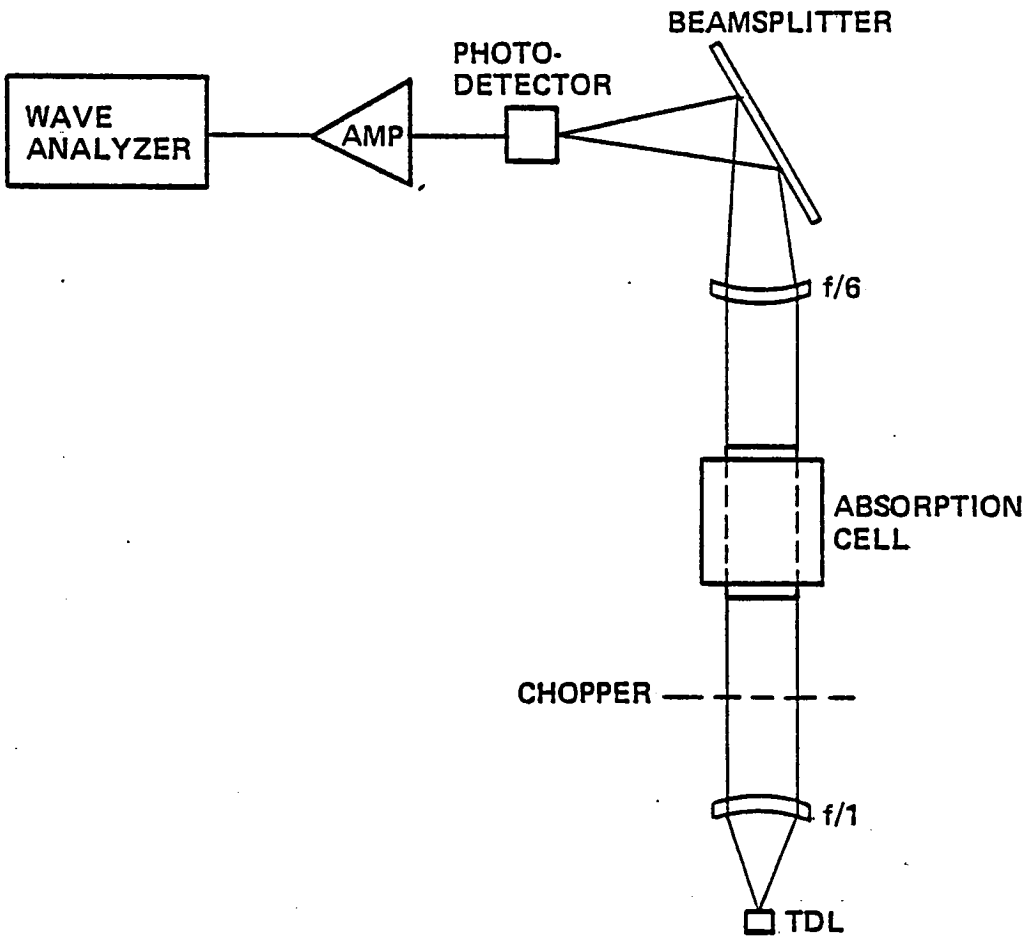

Figure 3-10. Optical Setup for Direct Detection of Absorption Line Shape.

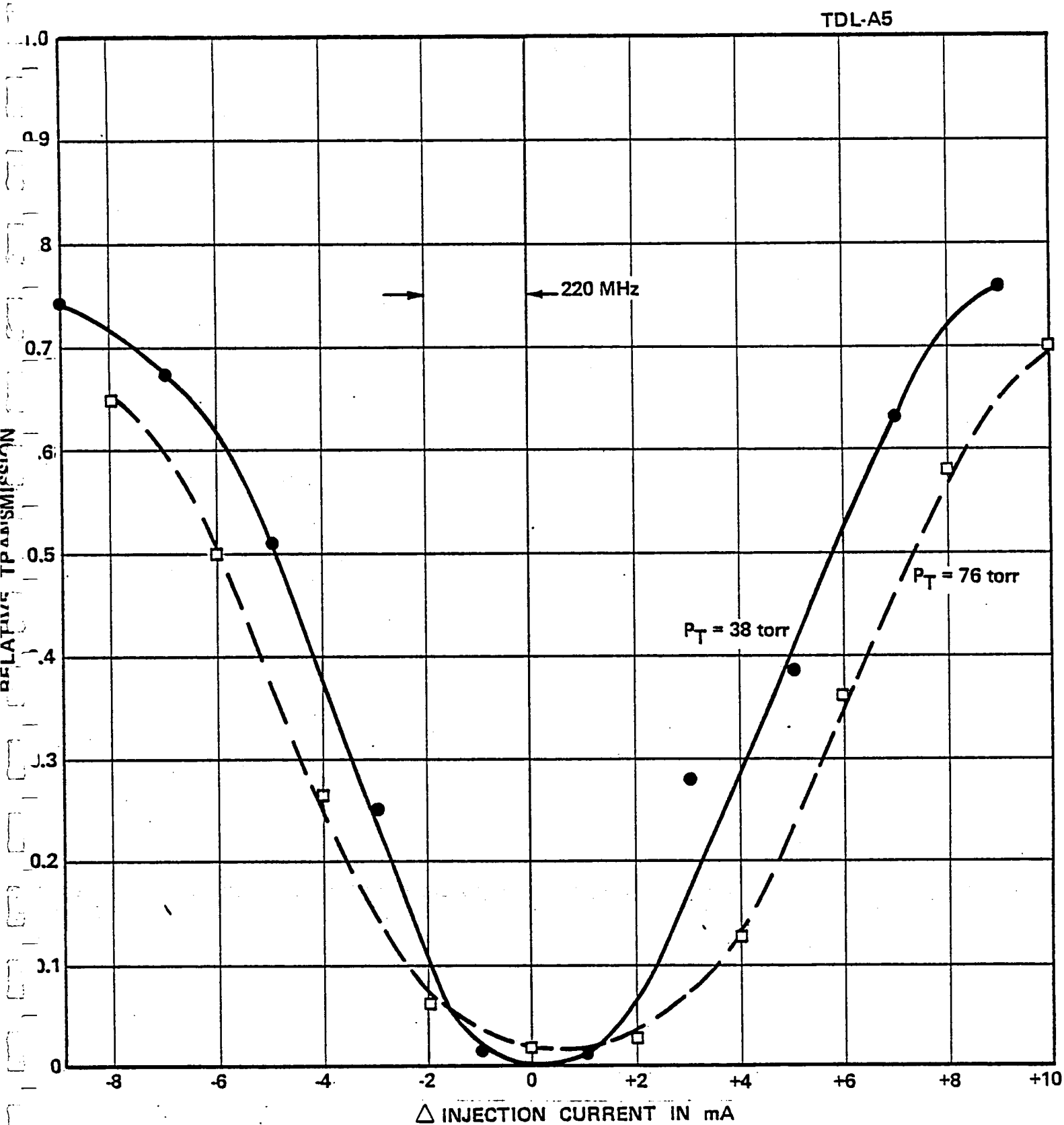

Figure 3-11. Ammonia Line Shapes Obtained Using a TDL Direct Detection Measurement Setup for P_{NH_3} = 0.5 torr, ν_o = 930.76 cm^{-1}, AND T = 57.9 K

and cell total pressures between 19 and 200 torr are given in Figure 3-12. The natural logarithm of the inverse of the transmission as a function of the ratio of the standard pressure, P_o, to the cell total pressure, P_T, is shown in this (semi-log) plot. The slope of the linear region is 0.46 and corresponds to cell total pressures which are greater than 75 torr.

Using the constants which are specified in Appendix A, a computer program has been developed which calculates the theoretical line shapes for the selected ammonia spectral line at $\nu_o = 930.76\ cm^{-1}$ and an effective video bandwidth of $B_v = 50$ MHz. As an example, the calculated ammonia line shape for $P_T = 38$ torr is given in Figure 3-13 for $P_{NH_3} = 0.5$ and 0.6 torr. The direct detection spectroscopic measurement data of Figure 3-11 has also been included for comparison. Two values of NH_3 partial pressure are included in Figure 3-13 to allow for the pressure measurement accuracy of $\pm$ 0.05 torr.

As can be seen, the measured spectral transmissions through the wings of the selected NH_3 signature line are lower than the calculated values. The measured and calculated half widths at half maxima for $P_T = 38$ and 76 torr are given in Table 3-2.

Table 3-2. DIRECT DETECTION MEASURED AND CALCULATED VALUES OF AMMONIA LINEWIDTH FOR $\nu_o = 930.76\ cm^{-1}$, $P_{NH_3} = 0.5$ TORR AND $B_v = 50$ MHz

Total Pressure (torr)	Half Width at Half Maximum (MHz) (Measured)	(Calculated)
38	~585	~350
76	~745	~468

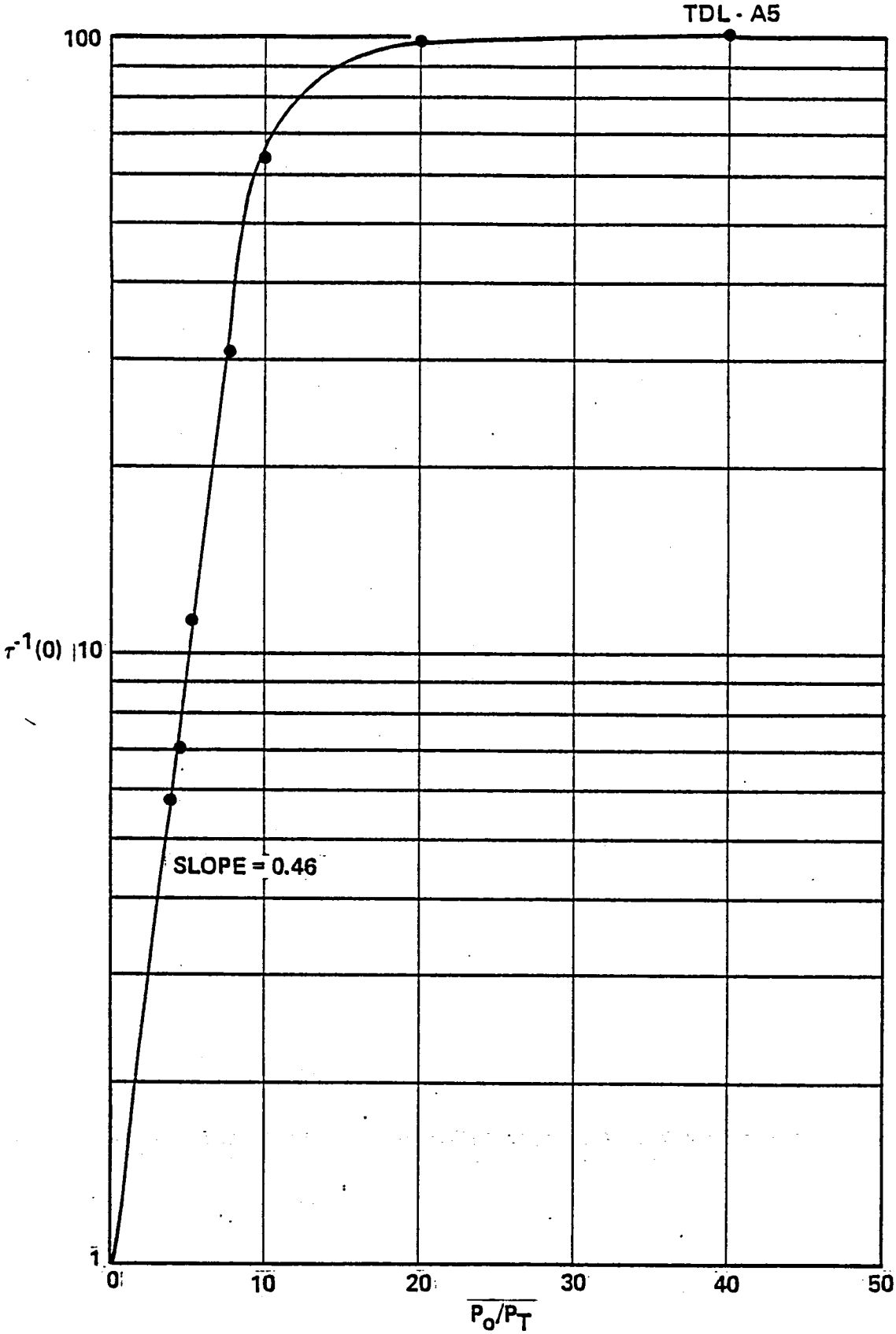

Figure 3-12. Measured Line-Center Transmission vs the Inverse of the Test Cell Total Pressure using a TDL Direct Detection Measurement Setup. P_{NH_3} = 0.5 TORR, ν_o = 930.76 cm^{-1}, AND T = 57.9 K

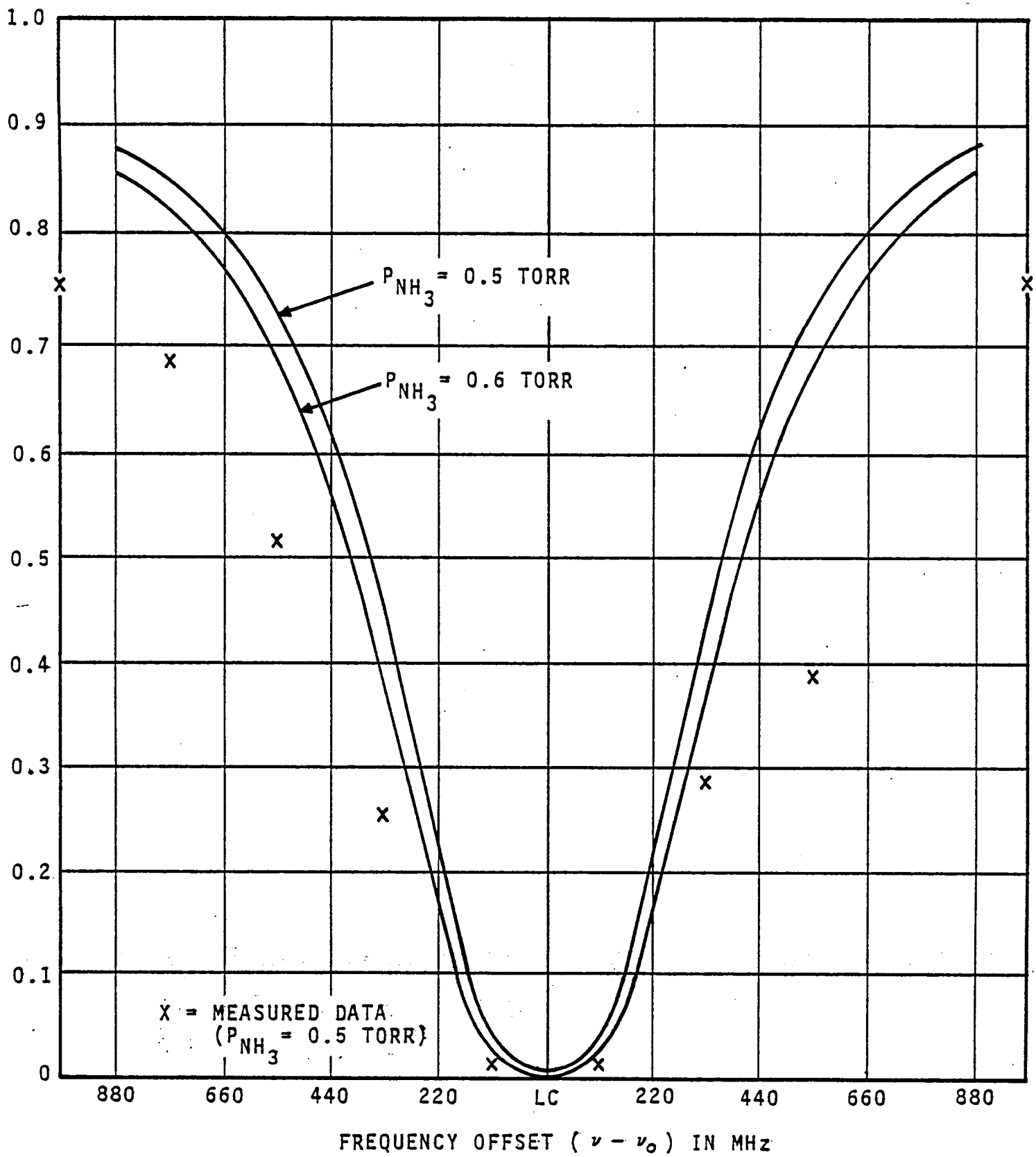

FIGURE 3-13. MEASURED AND CALCULATED AMMONIA ABSORPTION LINE SHAPE FOR A TOTAL PRESSURE OF 38 TORR, B_V = 50 MHz, AND ν_0 = 930.76 cm^{-1}

The calculated line center transmission at $\nu_o = 930.76$ is given in Figure 3-14 for $B_v = 50$ MHz and $P_{NH_3} = 0.5$ and 0.6 torr. The measured TDL data of Figure 3-12 has been included for comparison. The measured line center transmission data for $P_{NH_3} = 0.5$ torr appears to be in better agreement with the calculated data for $P_{NH_3} = 0.6$ torr.

Some possible causes for the discrepancies between the calculated and measured line profile data are discussed after the heterodyne spectroscopic measurement data is reviewed (see Section IV-D).

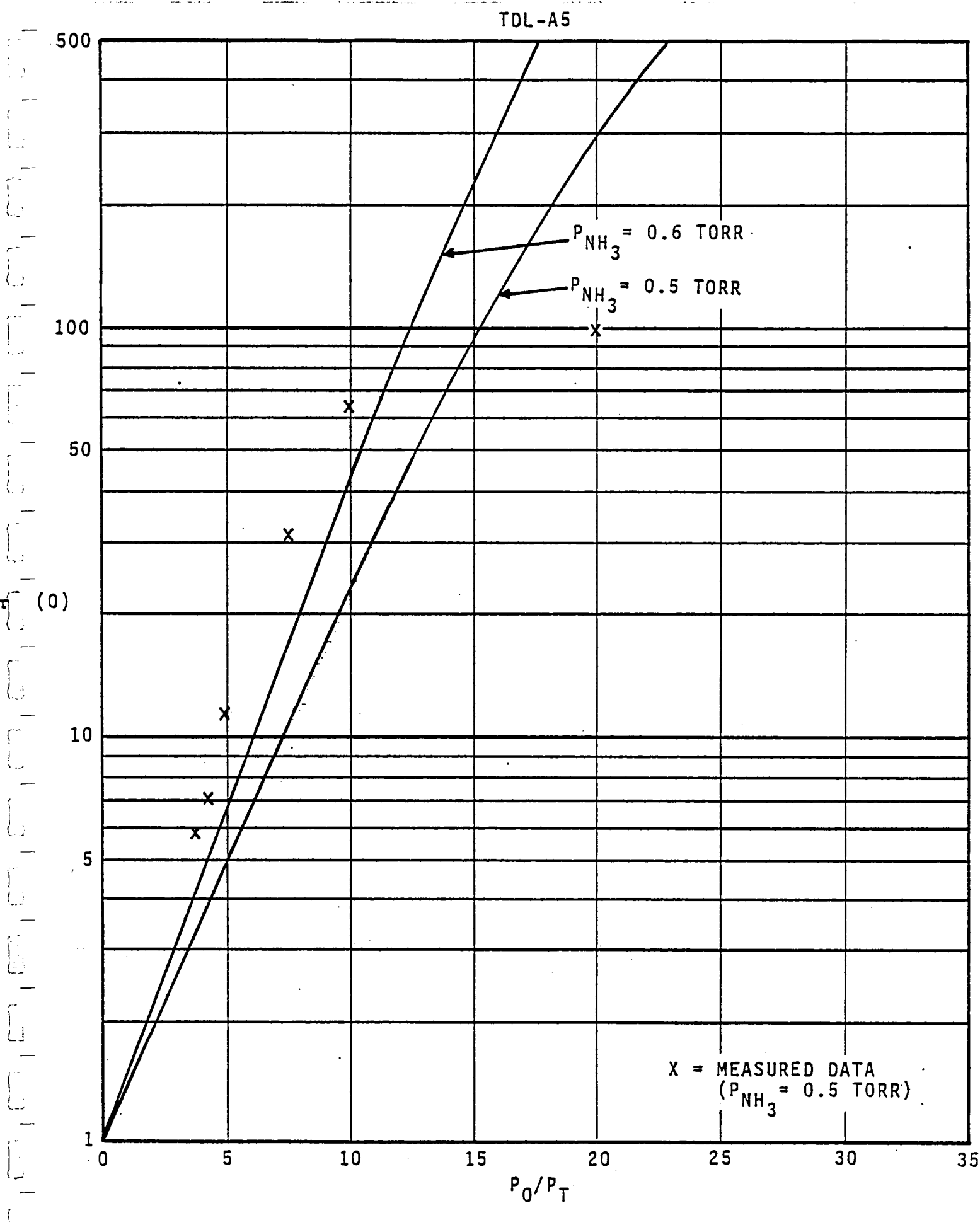

FIGURE 3-14. MEASURED AND CALCULATED AMMONIA LINE CENTER TRANSMISSION DATA FOR B_V = 50 MHz, ν_0 = 930.76 cm^{-1}

IV. HETERODYNE DETECTION MEASUREMENTS OF TUNABLE DIODE LASER

Heterodyne detection measurements which evaluate tunable diode laser local oscillators under laboratory conditions have been carried out. This section describes TDL frequency stability, heterodyne sensitivity and signal-to-noise ratio, and heterodyne spectroscopy of selected ammonia rotation-vibration spectral lines.

An analysis of heterodyne detection in photovoltaic mixer elements (Ref. 11) and high spectral resolution measurements using an infrared heterodyne radiometer (Refs. 12, 13, 14, and 15) have been previously reported. Infrared heterodyne radiometer measurements using TDL local oscillators have also been reported (Refs. 13, 16, and 17).

A. TDL Frequency Stability

In a heterodyne spectrometer the spectral resolution can be fixed by any of several factors. In practice the spectral stability of a laser local oscillator (LO) is expected to limit the overall spectral resolution of a heterodyne spectrometer. Theoretically the emission "linewidth" of a semiconductor laser is less than 3 MHz, however, several effects may increase the actual TDL emission profile. TDL temperature and current instabilities are believed to be two major causes of spectral broadening (see Figures 3-5 and 3-6). Since semiconductor lasers are also capable of being pressure tuned, any pressure waves propagated through the TDL device will also cause an increase in the emission linewidth and reduce the ultimate spectral resolution.

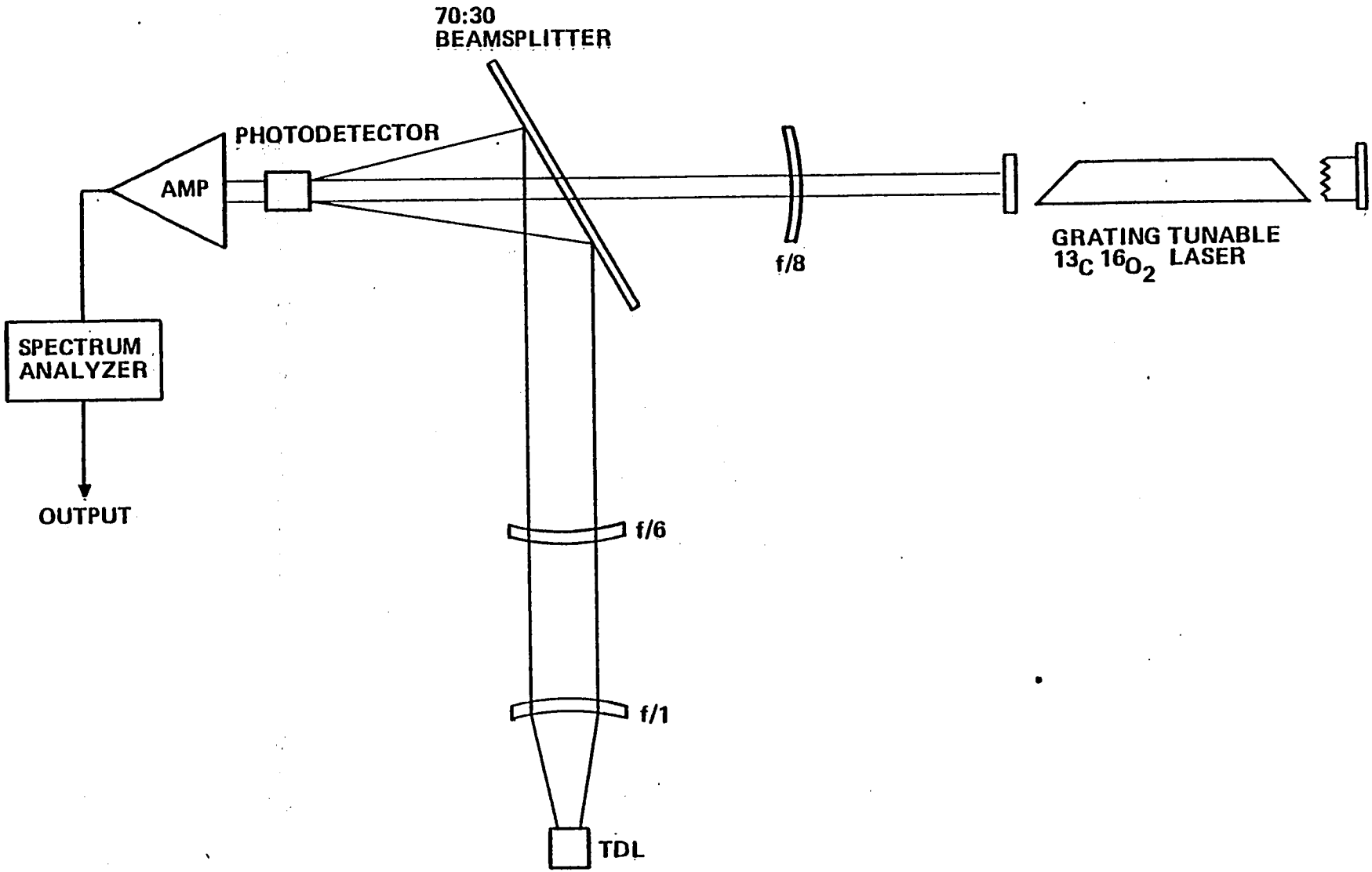

Figure 4-1. Measurement Setup to Evaluate Spectral Linewidth of a TDL

The heterodyne receiver setup used to evaluate the spectral linewidth of the TDL devices is shown in Figure 4-1. The output of a stable, sealed CO_2 gas laser illuminates the wideband HgCdTe photomixer and serves as the LO source while the TDL serves as the signal source. The previously measured short-term frequency stability of the CO_2 gas laser was approximately 200 kHz. Using temperature and current tuning the emission wavelength of the diode laser was adjusted to operate near the emission wavelength of the local oscillator laser (R18 transition of the $^{13}C^{16}O_2$ laser at 927.3 cm^{-1}).

The output beams of the two laser sources in the heterodyne measurement setup were spatially adjusted so that the laser radiation matched the active area of the photomixer. The IF output of the photomixer was amplified in a wideband ($\approx$2 GHz) preamplifier and examined using an RF spectrum analyzer (see Figure 4-1).

Four spectrum analyzer display photographs of the heterodyne receiver IF output spectrum are given in Figure 4-2. Figure 4-2A shows the measured IF spectrum for the case where the TDL spectral frequency (ν_s) falls below the CO_2 laser LO frequency (ν_{LO}) and Figures 4-2B, -2C, and -2D show the measured IF spectrum for the case of $\nu_s > \nu_{LO}$. Figures 4-2A and -2B have a horizontal scale of 100 MHz/cm with no IF offset. Figures 4-2C and -2D have a horizontal scale of 30 MHz/cm with an IF offset of 500 MHz. Figure 4-2D is a four exposure photograph with a total exposure time of one second. The TDL heat sink temperature and injection

TDL-A5
ν_{LO} = 927.3 cm^{-1}
T = 57.6K
I_o = 1 mA
I_S = 95 μA (I_o = 0)

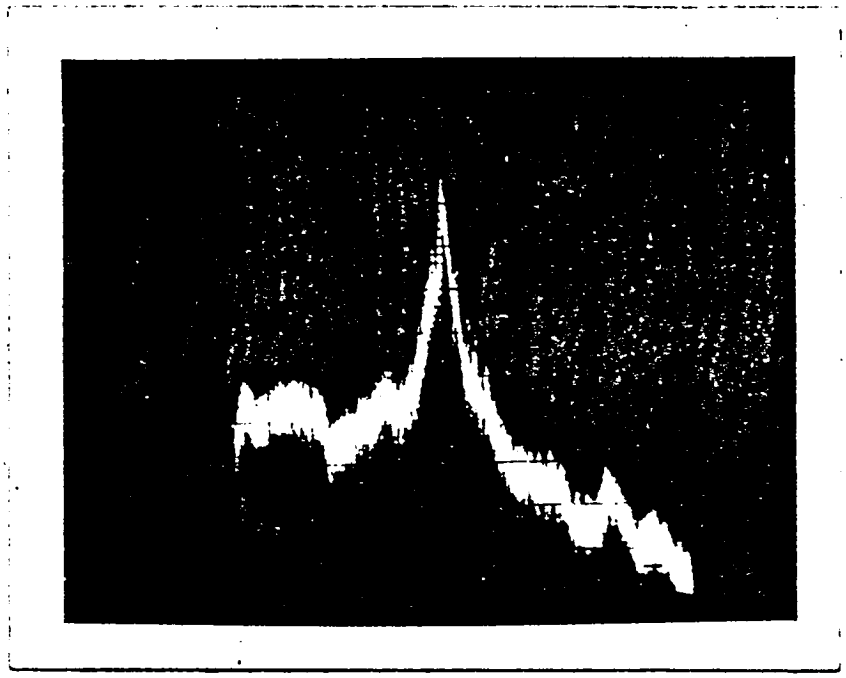

5 dB/cm

100 MHz/cm

A. I_{DC} = 1.5942 Amp

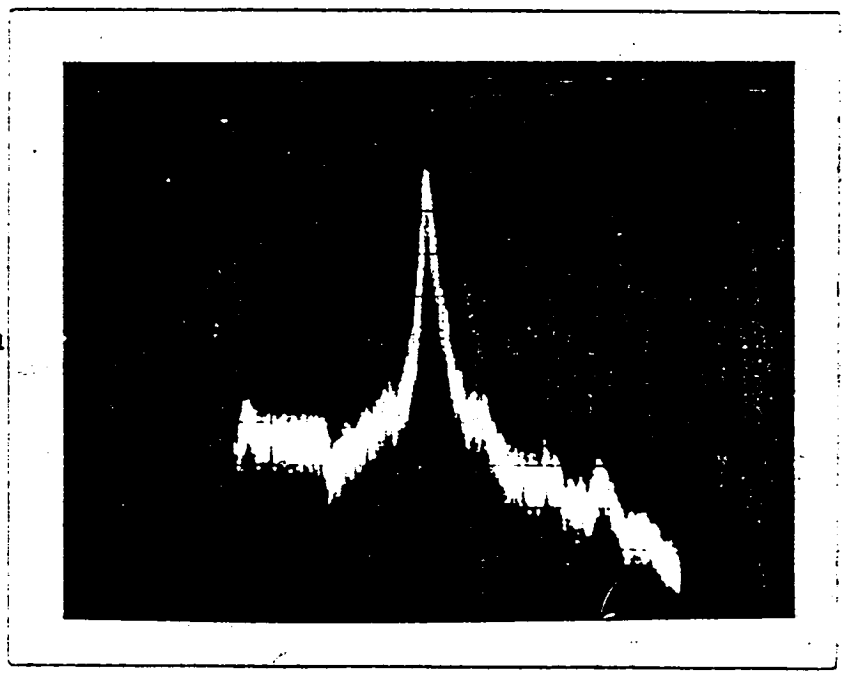

5 dB/cm

100 MHz/cm

B. I_{DC} = 1.6027 Amp

I_{DC} = TDL Injection Current
I_S = TDL Induced DC (P_{LO} = 0)

Figure 4-2. Measured IF Beat Frequency for TDL Signal and CO_2 Laser Local Oscillator (Page 1 of 2)

TDL-A5
ν_{LO} = 927.3 cm^{-1}
T = 57.6K
I_o = 1 mA
I_S = 95 μA

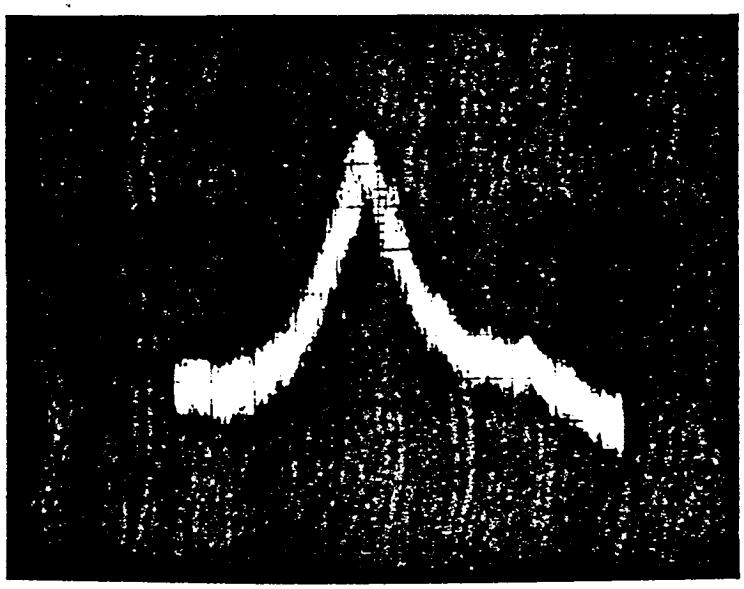

5 dB/cm

30 MHz/cm

C. I_{DC} = 1.6027 Amp (IF centered at 500 MHz)

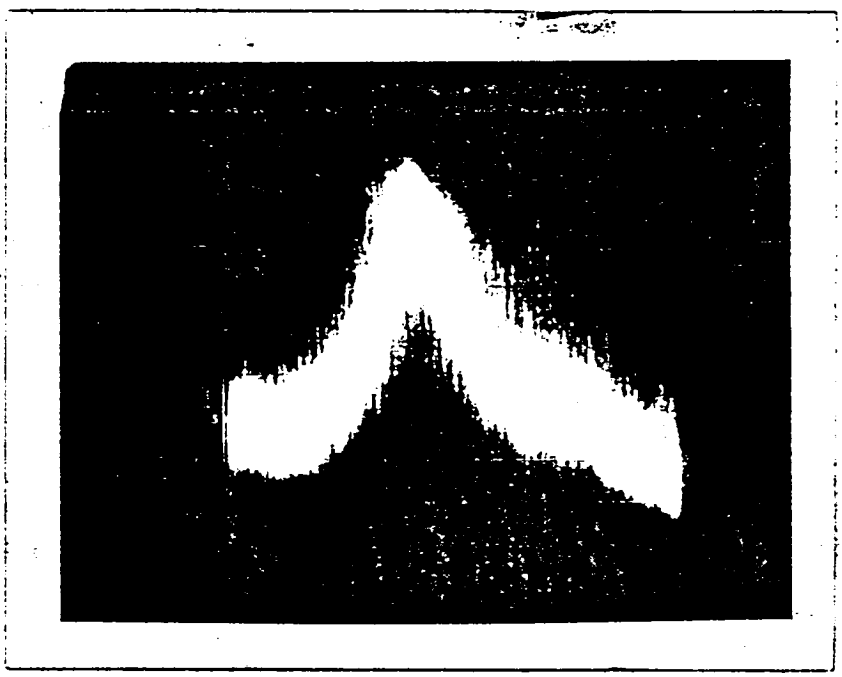

5 dB/cm

30 MHz/cm

D. One-Second Exposure for I_{DC} = 1.6027 Amp (IF centered at 500 MHz)

I_{DC} = TD Injection Current
I_S = TDL Induced DC Current (P_{LO}= 0)

Figure 4-2. Measured IF Beat Frequency for TDL Signal and CO_2 Laser Local Oscillator (Page 2 of 2)

currents are also indicated in Figure 4-2. The measured photo-induced mixer dc current (I_s = 95 μA) due to the TDL signal power for the case of no incident CO_2 laser power is also indicated in Figure 4-2. The measured value of I_s indicates that the incident TDL power level of approximately 50 μW is a factor of about ten smaller than the CO_2 laser LO power level.

An instantaneous TDL frequency stability of 10 MHz has been calculated based on the measured TDL data (Figures 3-4 and 3-5), provided the variations in I_{DC} and T are held to better than ± 50 microamperes and ± 0.25 millidegree Kelvin. The manufacturer's quoted values for the current and the temperature stabilities (± 30 microamperes and ± 1 millidegree Kelvin, respectively) are consistent with the requirements for the same overall TDL frequency stability of 10 MHz, or better. The apparent instantaneous (250 msec) frequency stability of TDL-A5 is approximately 30 MHz as measured at the half-power points in Figure 4-2C.

From equation (3-3) it is clear that small changes in the TDL's cavity length will give rise to changes in the emitted wavelength. Consequently the amplitudes of any spatial vibrations created in the TDL (by refrigerator operation, for example) must be minimized to maintain the best possible frequency stability.

The measured instantaneous frequency stability of the diode laser was not equivalent to the short term stability. As can be observed in Figure 4-2D, the diode's frequency varied about ± 45 MHz in a time period of one second. A frequency jitter of over 140 MHz has been observed in a two-second period. These large

variations were not caused by a random noise process but are believed to have been the result of vibrations induced in the TDL by the piston action of the cooler. The piston oscillates at a frequency of two to three hertz; the resulting shocks are obviously the cause of the poor frequency stability since the wide variations could be eliminated by turning off the refrigerator. Clearly, then, some form of vibration isolation of semiconductor lasers is required in order to achieve the full potential of these devices. Several methods of isolation have been attempted with some recent work (Refs. 18 and 19) indicating attainable short term frequency stabilities of better than 5 MHz.

Since the frequency deviation caused by the piston is not uniformly distributed in time, an electronic technique which minimizes its effect on certain systems may offer the possibility of improved overall spectral stability. Data collected during times of severe LO frequency deviation is normally integrated with the data collected under the condition of an undisturbed LO frequency. It may be possible to prevent the integration of the undesired data by electronic blanking techniques.

Some investigators (Ref. 4) have noted TDL wavelength changes with time that have been attributed to changes in element stoichiometry. It is possible that these changes may have been caused by cycling of the devices between cryogenic and room temperatures. Of the two TDLs evaluated on this program preliminary results indicate that TDL-A5 has shown excellent repeatability over a time period of a few months with six temperature cycles while TDL-A6, having undergone identical

thermal cycling, has shown signs of a significant variation of its output parameters. For example, spectral overlap of TDL-A6 with a particular CO_2 laser transition could not be repeated after several temperature cycles although the TDL's total output power did not exhibit any significant variation.

It should be noted that the accuracy with which particular values of temperature and injection current may be reset has an effect on the apparent wavelength repeatability. In practice, the temperature sensor in the cooler should be mounted as close as possible to the TDL element in order to minimize the effect of temperature differences which may be caused by any intervening thermal resistance. This thermal resistance is a function of time since it is expected to increase as the vacuum insulation of the dewar deteriorates.

In summary, since the position and spacing of the wavelength modes are determined by the TDL stoichiometry and geometry, the wavelength stability and repeatability should be limited primarily by the accuracy with which the junction temperature and injection current can be controlled. Using the commercially available cooler and current power supply an instantaneous (250 msec) TDL spectral stability of approximately 30 MHz has been observed.

B. Heterodyne Sensitivity Using Multi-Mode TDL Local Oscillator

Heterodyne receiver sensitivity measurements have been carried out using a multi-mode TDL local oscillator. A TDL can simultaneously emit two or more wavelengths at specific temperature (and current) values. For example, when cooled to T = 50.23 K, TDL-A5 emitted two wavelength modes at I_{DC} = 1.10 amperes, three wavelength modes at I_{DC} = 1.5 amperes and four wavelength modes at I_{DC} = 1.48 amperes

(see Figure 3-4). Generally these multi-mode emissions are most numerous under high current conditions. Under maximum current conditions, multiple continuous emission bands of approximately 0.3 cm^{-1} width and separated by the typical mode spacing have been observed. Such bands are probably evidence of bounce modes in the optical cavity and filamentary lasing operation.

A simplified representation of a heterodyne receiver that employs a TDL LO which emits three independent wavelength modes is given in Figure 4-3. The heterodyne receiver examines a broadband thermal source (P_{source}) with the objective of measuring a single vibrational-rotational spectral line at $\nu = \nu_p$ which is in spectral proximity to one of the TDL wavelength modes. Both the source and the TDL radiation are coupled onto the photomixer and the resulting IF difference frequency is amplified in an IF amplifier having a gain, G, and a bandwidth, B_{IF}. The presence of the three TDL wavelength modes at ν_1, ν_2, and ν_3 results in a situation in which the heterodyne receiver examines three spectral regions of the source radiance (see Figure 4-3C). Although only one of the spectral regions overlaps the spectral line of interest heterodyne receiver noise exists in all three spectral regions and causes a reduction in the overall heterodyne receiver sensitivity.

In addition, the IF difference wavelengths may beat together in a double conversion mode; should $|f_b - f_a| < B_{IF}$ saturation of the photomixer IF output may result. To study such TDL self-beating effects photographs have been made of the spectrum analyzer display of the wideband photomixer IF output with the mixer illuminated by a TDL LO (see Figure 4-4). The TDL injection current and temperature

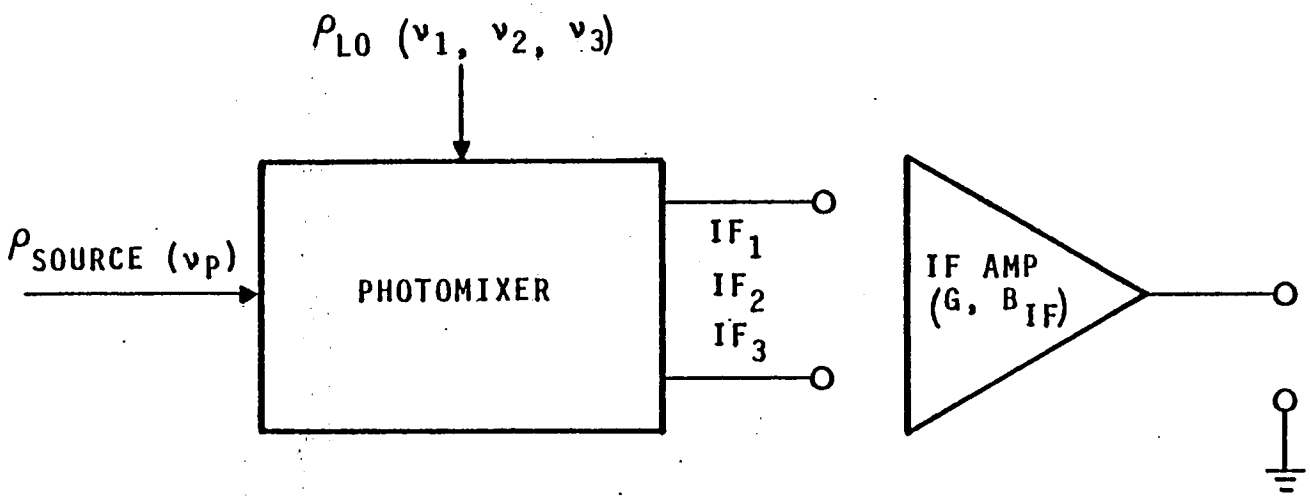

A. SIMPLIFIED HETERODYNE RECEIVER REPRESENTATION

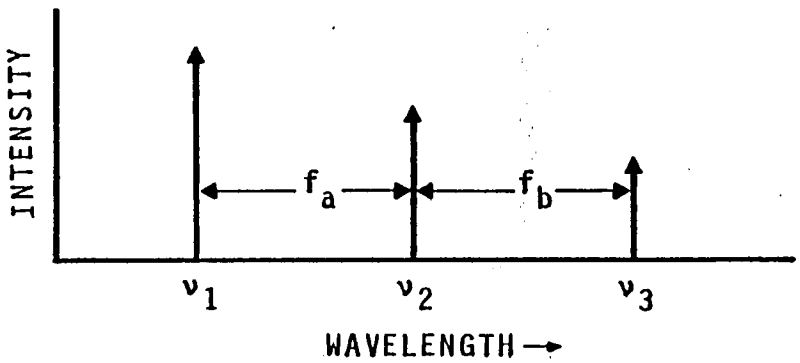

B. TDL MULTIMODE OUTPUTS

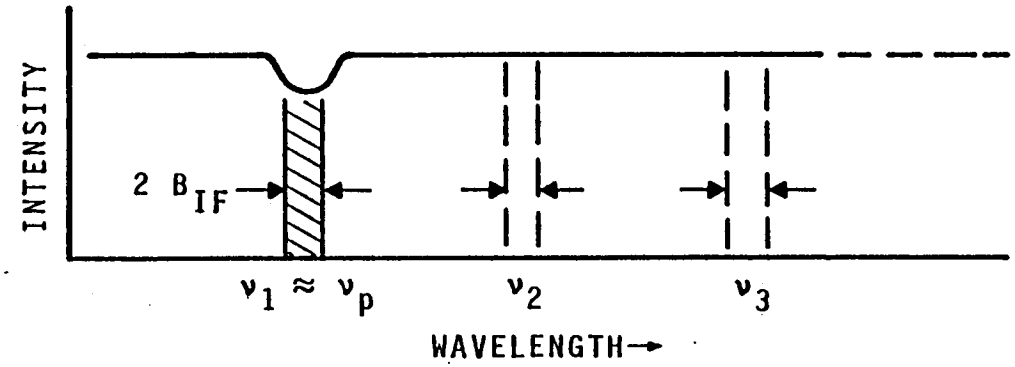

C. HETERODYNE RECEIVER SPECTRAL RESPONSE

FIGURE 4-3. SIMPLIFIED REPRESENTATION OF A HETERODYNE RECEIVER EMPLOYING A MULTI-MODE TDL LOCAL OSCILLATOR

TDL-A5
T = 57.6K
I_{DC} = 1.5739 Amp

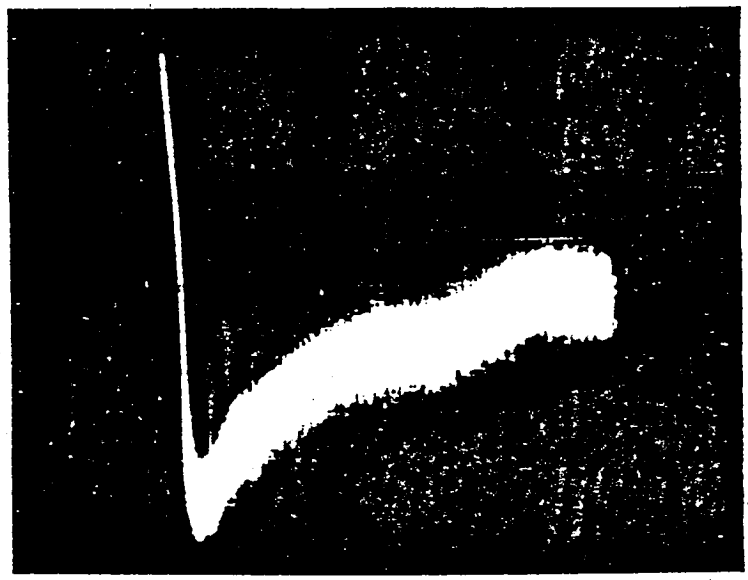

5 dB/cm

10 MHz/cm

A. Reference Background Level (I_o = 0)

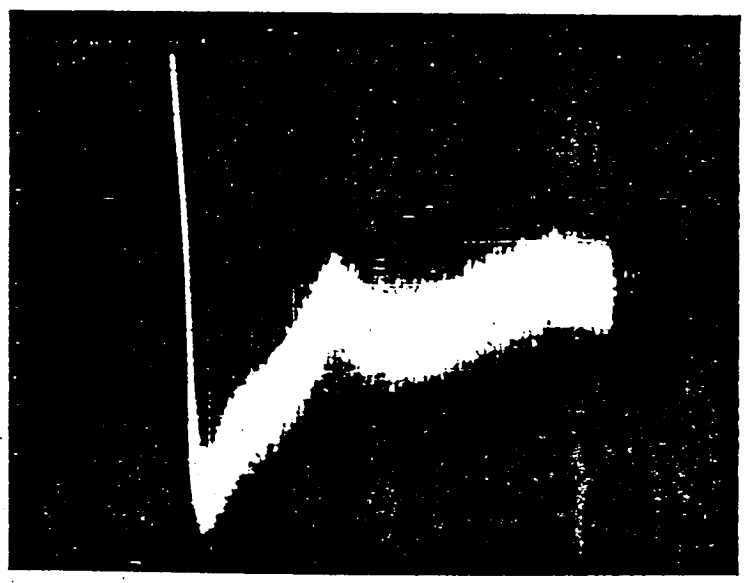

5 dB/cm

10 MHz/cm

B. Measured Photomixer Output (I_o = 40 μA)

Figure 4-4. Measured Photomixer IF Spectral Output When Illuminated by a Multimoding Diode Laser LO (Page 1 of 2)

TDL-A5

T = 57.6K

I_{DC} = 1.5842 Amp

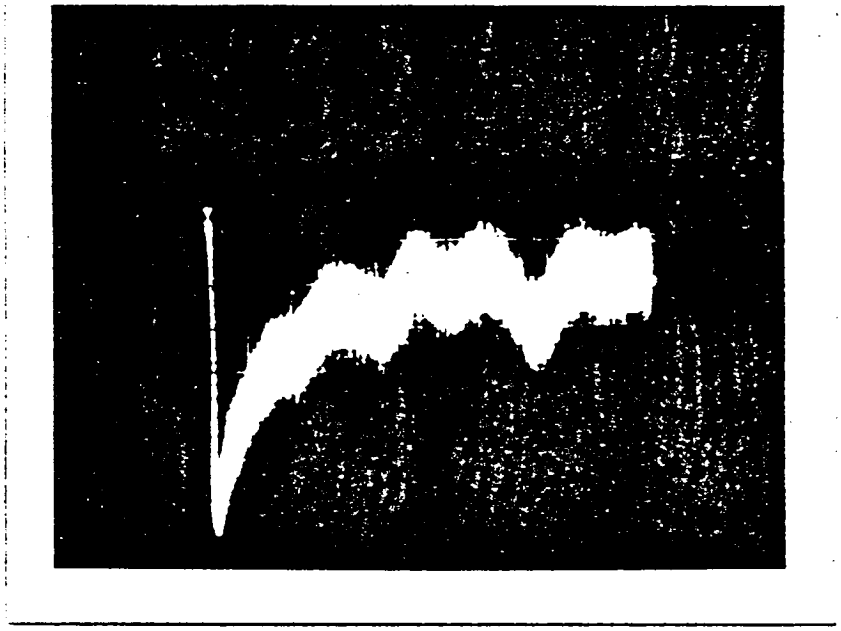

5 dB/cm

30 MHz/cm

C. Reference Background Level (I_o = 0)

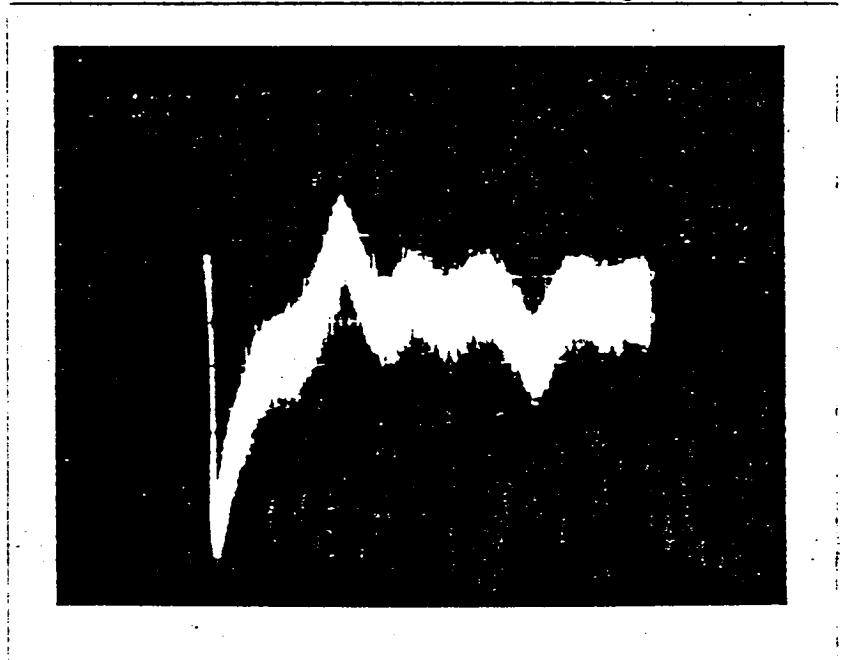

5 dB/cm

95 MHz

30 MHz/cm

D. Measured Photomixer Output (I_o = 65 μA

Figure 4-4. Measured Photomixer IF Spectral Output When Illuminated by a Multimoding Diode Laser LO (Page 2 of 2)

conditions were identical to those employed for the spectral tuning measurements described in Figure 3-5: the reference levels for IF frequencies between 0 and 100 MHz (and 0 and 300 MHz) are given in Figures 4-4A and 4-4C.

With the TDL LO beam illuminating the photomixer a spike which was 8 dB above the reference background noise level at IF = 36 MHz spontaneously appeared as the TDL current was increased to I_{DC} = 1.5739 ampere (see Figure 4-4B). Further increase of the injection current to 1.5842 ampere caused a gradual reduction of the spike at 36 MHz with a simultaneous creation of a 12 dB spike at 96 MHz (see Figure 4-4D). This IF spike was then continuously current-tunable out to an IF of 150 MHz at I_{DC} = 1.6076 ampere.

The IF spikes occurred in a region of triple wavelength output of the diode laser (see Figure 3-5). It should also be noted that the triple emission outputs dropped to only a double TDL frequency mode in the region where the video peak disappeared (I_{DC} = 1.6076). The cause of these comparatively low frequency video peaks is not known at this time. Since the frequency difference between laser modes is of the order of 50 GHz, it is possible that some form of double mixing with consequent secondary beat frequencies is the cause of this low frequency behavior; Further study of these phenomena is required.

Another form of TDL self-beating is illustrated in Figure 4-5 for the conditions of I_{DC} = 1.7100 ampere and I_o = 82 μA ($P_{LO} \approx$ 40 μW). Comparing Figure 4-5 with Figure 4-4C it is apparent that the level

TDL-A5
T = 57.6K

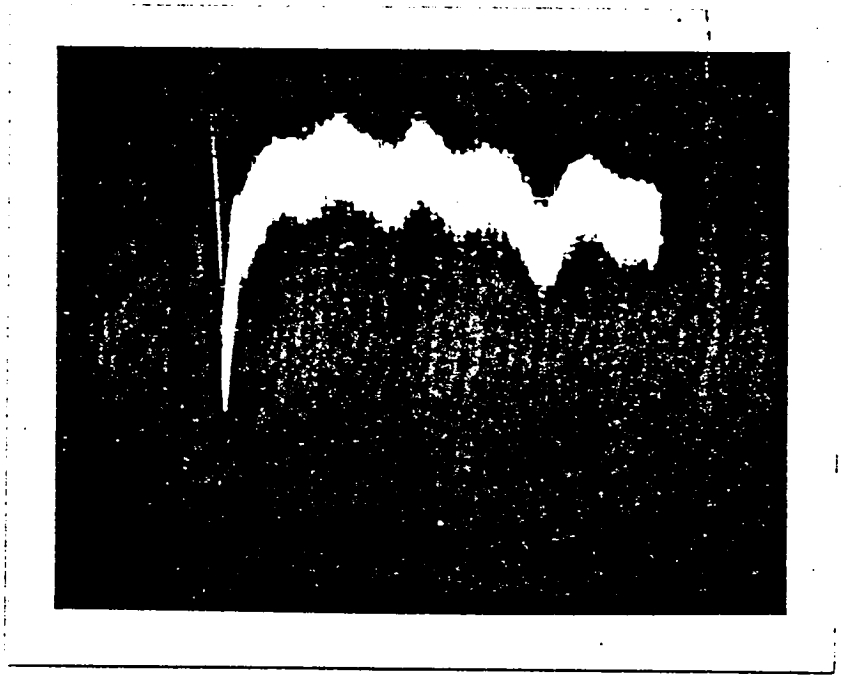

5 dB/cm

30 MHz/cm

I_{DC} = 1.7100 Amp
I_o = 82 μA

Figure 4-5. Measured Photomixer IF Spectral Output When Illuminated by a Multimoding Diode Laser

of the entire photomixer IF response has increased by 20 to 25 dB. From Figure 3-5 it can be seen that the diode laser was simultaneously emitting three wavelengths at I_{DC} = 1.71 ampere. One difference between the conditions in Figure 4-5 and those prevailing for Figure 4-4 was that one of the three modes (i.e., at ν = 927.57 cm^{-1}) disappeared at I_{DC} = 1.61 A and reappeared at I_{DC} = 1.71 A. Due to the very different effect on the IF response, the character of the diode laser output must have been different from the output noted previously. Further study is required to establish the stability and usability of TDLs in this modal transition region.

Spectral responses similar to those depicted in Figure 4-4 were observed in the triple mode region between I_{DC} = 1.76 A and I_{DC} = 1.80 A. However yet another form of TDL self-beating was noted at I_{DC} = 1.8862 ampere (I_o = 100 μA and $P_{TDL} \approx$ 50 μW) as shown in Figure 4-6. The data in Figure 4-6 indicate that a continuous band of beat frequencies can exist under certain TDL conditions. The width of the band was observed to vary, depending on I_{DC}, between 375 MHz and at least 2000 MHz. From Figure 3-5 it can be observed that the laser outputs in the region of I_{DC} = 1.8862 ampere and ν = 933.75 cm^{-1} are unusually close together. Such proximity may be the result of a bounce mode off the walls of the optical cavity or filamentary lasing. The closely spaced TDL outputs (perhaps a band output) when incident on the photodetector may undergo the possible double mixing process resulting in the observed spectrum.

TDL-A5
T = 57.6K

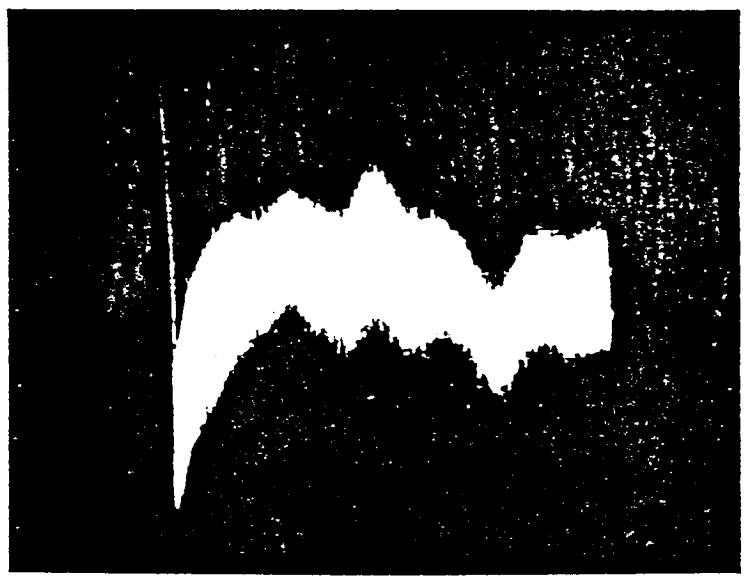

5 dB/cm

30 MHz/cm

I_{DC} = 1.8862 Amp
I_o = 100 μA

Figure 4-6. Measured Photomixer IF Spectral Output When Illuminated by a Multimoding Diode Laser

While the video response of the photodetector is corrupted by these unusual effects it must be noted that the heterodyne sensitivity of any system using this TDL as an LO will be severely degraded. If the wavelength of interest lies in a region of such multiple frequency output it is apparent that no accurate spectroscopic measurement can be performed. However, if the mechanism of the anomalous spectral response is located at the photomixer then suitable wavelength selection techniques which reject the undesired wavelengths may permit operation with a multi-wavelength mode diode laser.

C. Heterodyne Receiver Signal-to-Noise Ratio

A series of heterodyne receiver signal-to-noise ratio measurements using a TDL as a LO source was carried out. The heterodyne receiver sensitivity for a reverse biased photovoltaic photomixer is given (Ref. 12) by:

$$NEP(f) = \frac{h\nu}{\eta}\left\{1 + \frac{2k(T_m+T'_{IF})\ G_D}{qI_o}\left[1 + (f/f_c)^2\right]\right\} = \frac{h\nu}{\eta'} \quad (4\text{-}1)$$

where NEP(f) is the IF frequency-dependent noise equivalent power, $h\nu$ is the photon energy, T_m is the photomixer temperature, T'_{IF} is the effective input noise temperature of the IF preamplifier, G_D is the reverse shunt conductance of the photomixer, I_o is the LO induced photocurrent, q is the electronic charge, and f_c is the 3-dB cutoff frequency of the photomixer. For convenience these latter terms are grouped into an effective receiver quantum efficiency η'. The receiver sensitivity, NEP, is given by:

$$NEP = \frac{h\nu}{\eta'} B \qquad (4\text{-}2)$$

The IHR postdetection signal-to-noise ratio (SNR) for an extended thermal source is given by:

$$SNR = \frac{P_s \alpha (B\tau)^{1/2}}{NEP\ K} = \frac{P_s \eta' \alpha (B\tau)^{1/2}}{h\nu BK} \qquad (4\text{-}3)$$

where P_s is the power received from the thermal source within the diffraction limited IHR field of view, contained in a spectral window of extent 2B, and of correct polarization for heterodyne detection. K is the sensitivity constant (2 for a 50-percent Dicke-type radiometer), τ is the postdetection integration time constant of an ideal integrator, and α is the transmittance of the media and optics between the thermal source and the infrared photomixer.

When observing a thermal source of temperature T_s the heterodyne radiometer SNR is given by:

$$SNR = \frac{\eta' \alpha (B\tau)^{1/2}}{e^{h\nu/kT_s} - 1}, \quad f_c > B \qquad (4\text{-}4)$$

where k is Boltzmann's constant.

A simplified Dicke-switched heterodyne radiometer which employs a variable temperature blackbody as an infrared source and a tunable diode laser as a LO is depicted in Figure 4-7. A gas-absorption test cell is incorporated into the signal path to permit high resolution spectroscopic measurements. Measurement of the system signal-to-noise ratio using either a diode laser or a CO_2 gas laser as the photomixer LO for various levels of applied LO power was performed; the results are presented in Table 4-1.

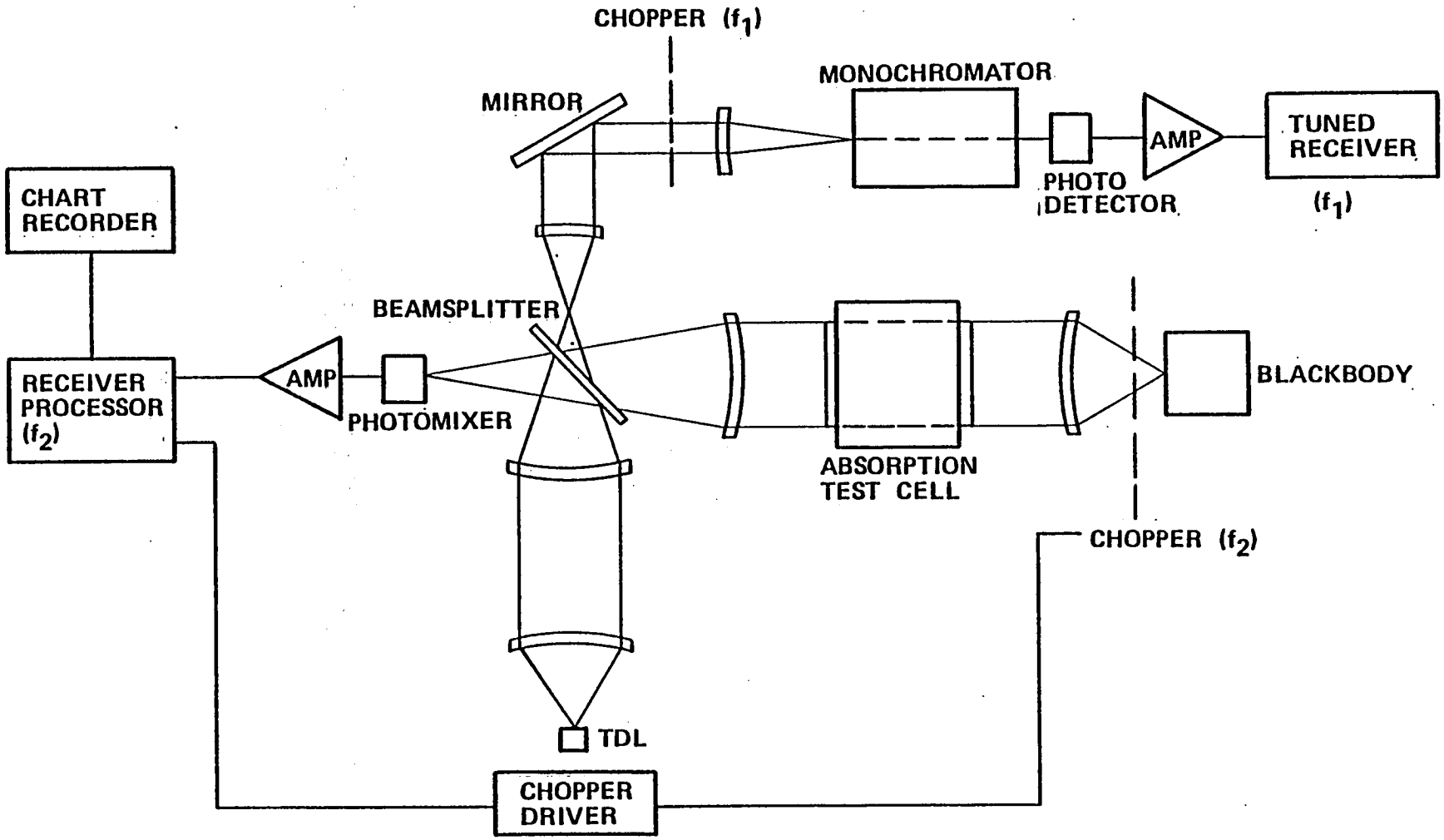

Figure 4-7. Heterodyne Receiver Measurement Setup Employing a TDL Local Oscillator

Table 4-1. Heterodyne Spectrometer Signal-to-Noise Measurements For Several Values of Laser LO Power for Blackbody Source Temperature of T = 1250K, IF Bandwidth $B = 10^8$ Hz and Integration Time of τ = 30 Seconds

CO_2 Laser Induced I_o (μA)	Measured SNR	Single Mode TDL Induced I_o(μA)	Measured SNR
25	4	-	-
40	-	40	2.5
50	8	-	-
100	14	-	-
200	21	-	-

Using equation (4-1) the calculated heterodyne radiometer SNR versus the photoinduced mixer current with the radiometer quality factor ($\alpha\eta\sqrt{B\tau}$) as a parameter is given in Figure 4-8 for the case of T_s = 1250K, ν = 927.3 cm^{-1}, and K = 2. As expected the heterodyne radiometer's SNR increases with increasing photoinduced photomixer current (i.e., increasing applied laser LO power). The SNR asymptotically approached a value for $I_o > 5$ mA for the particular test setup used for the reported measurements. As can be seen from Figure 4-8 the measured heterodyne SNR for the case of the CO_2 laser LO (Table 4-1) corresponds to a radiometer quality factor of $\alpha\eta\sqrt{B\tau} \approx$ 214. It should be noted that no particular attempt was made to optimize the optical efficiency or the thermal noise contribution of the wideband IF preamplifier.

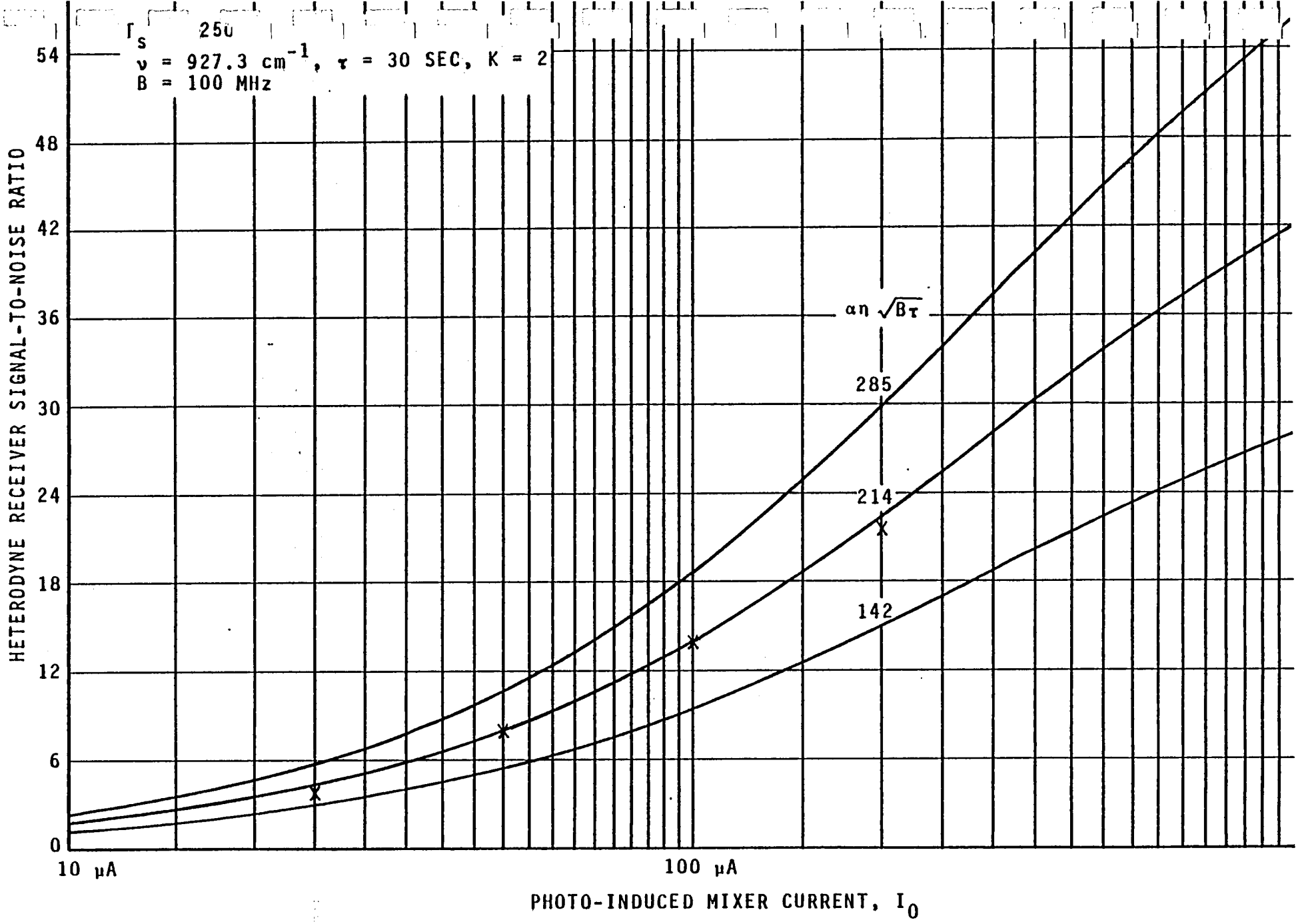

FIGURE 4-8. MEASURED AND CALCULATED HETERODYNE RADIOMETER SIGNAL-TO-NOISE RATIO AS A FUNCTION OF PHOTOINDUCED MIXER CURRENT WITH RADIOMETER QUALITY FACTOR AS A PARAMETER

The measured radiometer SNR of 2.5 for the TDL LO with I_o = 40 μA (P ≈ 20 μW) is a factor of approximately 2.6 below the measured value for a CO_2 laser LO with the same amount of photoinduced mixer current. The difference between the radiometer performance with a TDL LO and the performance with a CO_2 laser LO may be due to such factors as: (1) less uniform TDL phase fronts, (2) poorer TDL collimation, (3) larger amounts of frequency and amplitude noise, and/or (4) nonuniform spatial distribution of the TDL beam.

Further measurements are required to identify the primary causes of the degradation in performance of heterodyne radiometers using TDL local oscillators.

D. Heterodyne Spectroscopic Measurements of Selected Absorption Lines

The piece-wise continuous tuning nature of the diode laser limits heterodyne measurements to ammonia absorption lines for which a spectral overlap can be obtained, while the relatively short test cell limits the measurements to ammonia lines with absorption coefficients which are greater than approximately 5×10^{-20} cm^2 mol^{-1} cm^{-1}. The aQ (3,3) absorption line in the Q branch of the ν_2 vibration-rotation band at ν_o = 930.76 cm^{-1} (Ref. 10) was used for all of the measurements.

Heterodyne measurements of the absorption line profile were carried out for different partial pressures of ammonia, P_{NH_3}, as well as various total cell pressures, P_T; results are given in Figures 4-9 and 4-10 for ammonia partial pressures of 0.1 and 0.5

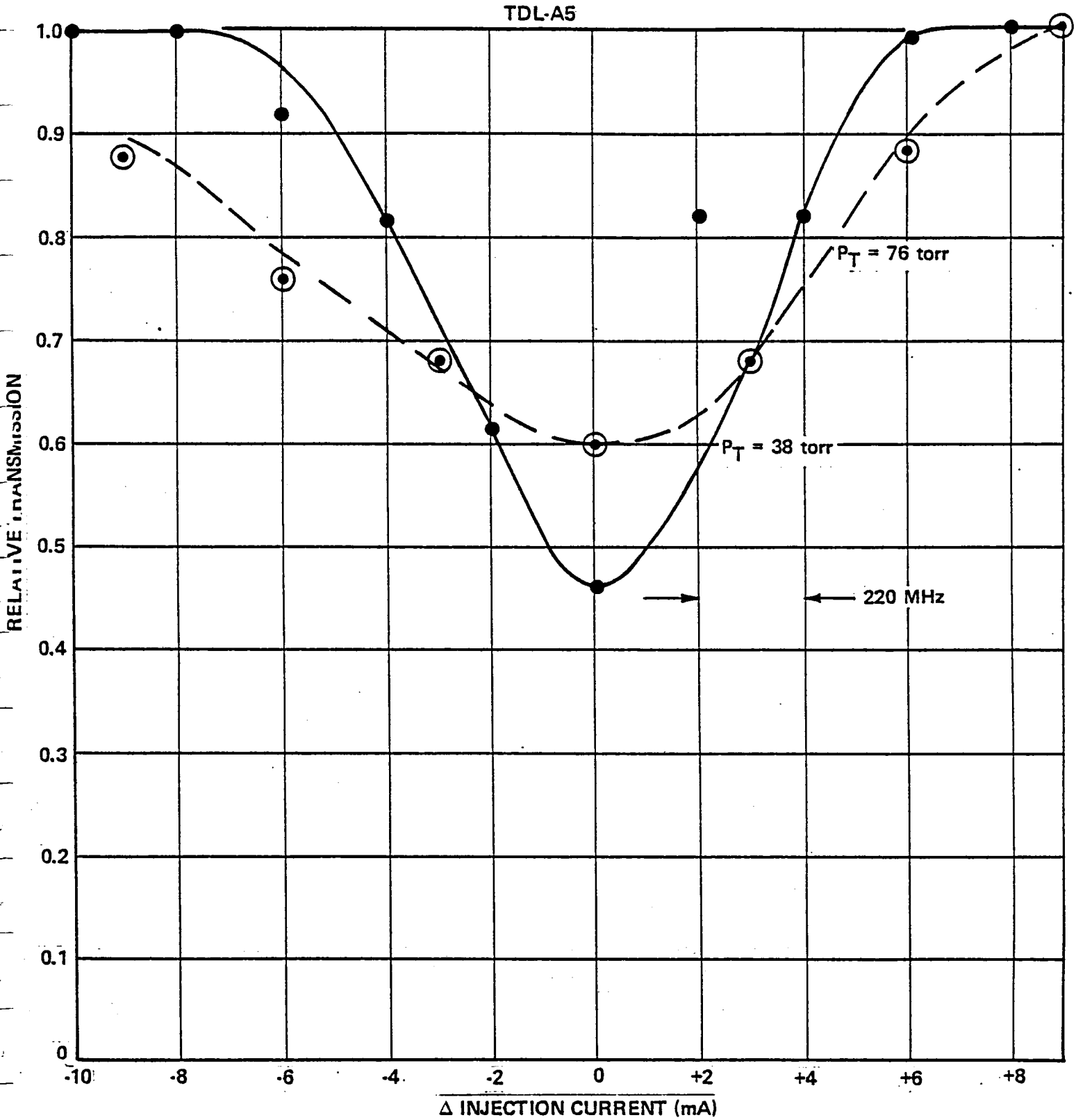

Figure 4-9. Ammonia Spectral Lineshape Obtained Using a TDL Heterodyne Measurement Setup for P_{NH_3} = 0.1 torr, T = 57.9 K, and ν_0 = 930.76 cm^{-1}.

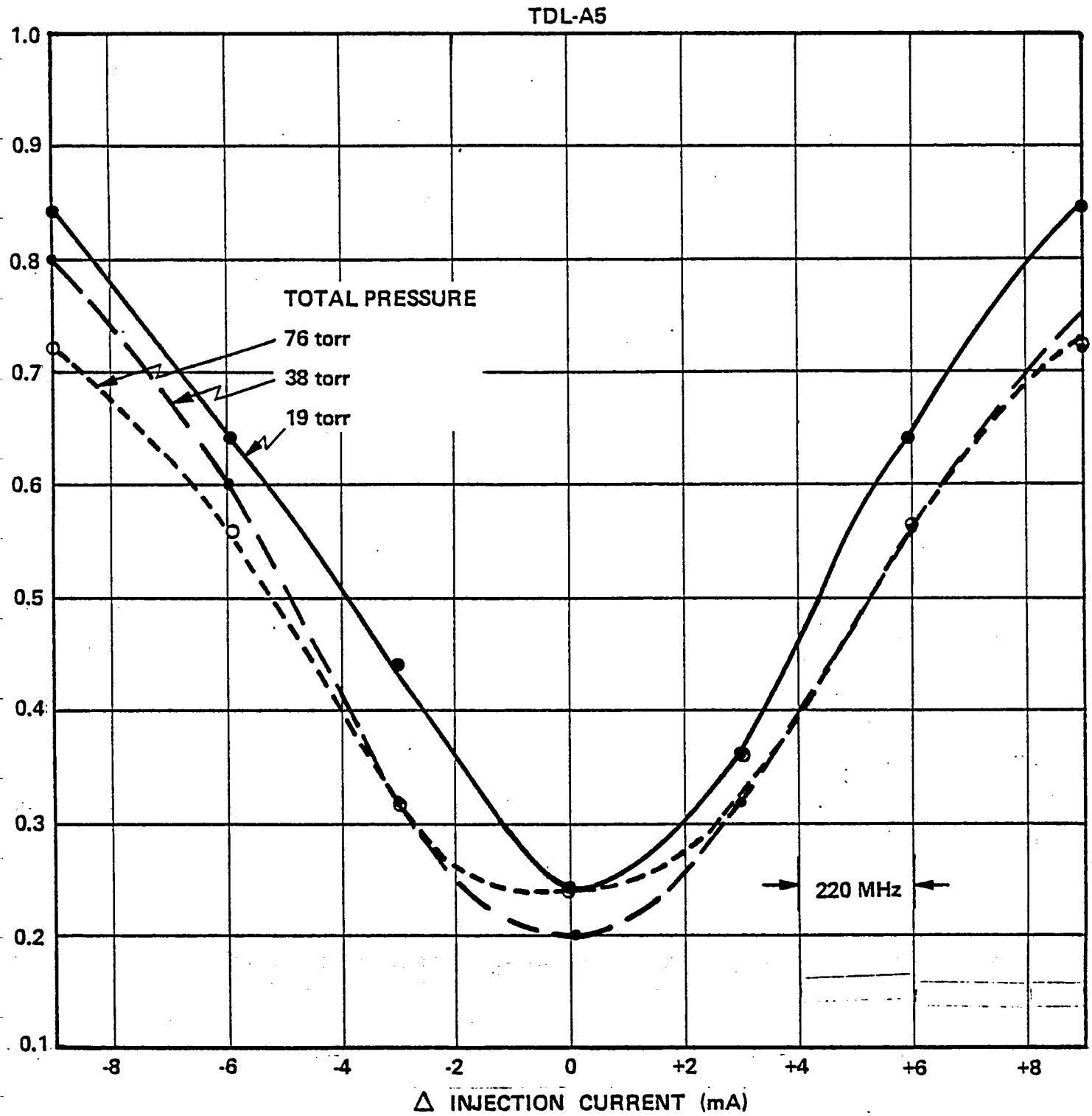

Figure 4-10. Ammonia Spectral Lineshapes Obtained Using a TDL Heterodyne Measurement Setup for P_{NH_3} = 0.5 torr, T = 57.9 K, AND ν_o = 930.76 cm^{-1}

torr and total pressures between 19 and 76 torr. The measured half widths at half maxima of the ammonia spectral lines varied between 350 MHz for P_{NH_3} = 0.1 torr and P_T = 38 torr, and 735 MHz for P_{NH_3} = 0.5 torr and P_T = 76 torr. As expected, the absorption linewidth increased with increasing cell total pressure.

Heterodyne measurements of the line center transmission, $\tau(o)$, for NH_3 partial pressures of 0.1 and 0.5 torr and cell total pressures between 38 torr and 750 torr are shown in Figure 4-11. The inverse of the line center transmission as a function of the ratio of the standard pressure, P_o, to the cell total pressure, P_T, is shown in the (semi-log) plot. The linear regions of the curves exhibit slopes of 0.096 (for P_{NH_3} = 0.1 torr) and 0.133 (for P_{NH_3} = 0.5 torr) for total pressures greater than 76 torr.

The theoretical NH_3 line shapes have been developed using a receiver bandwidth of B = 150 MHz. This value is representative of the single-sideband envelope where the full bandwidth of the TDL local oscillator does not exceed 100 MHz.

The calculated shapes of the ammonia line at ν = 930.76 cm^{-1} for P_T = 38 torr and the selected values of P_{NH_3} are given in Figures 4-12 and 4-13. The measured data of Figures 4-9 and 4-10 are also included for comparison. The measured and calculated half widths for P_{NH_3} = 0.1 torr are given in Table 4-2.

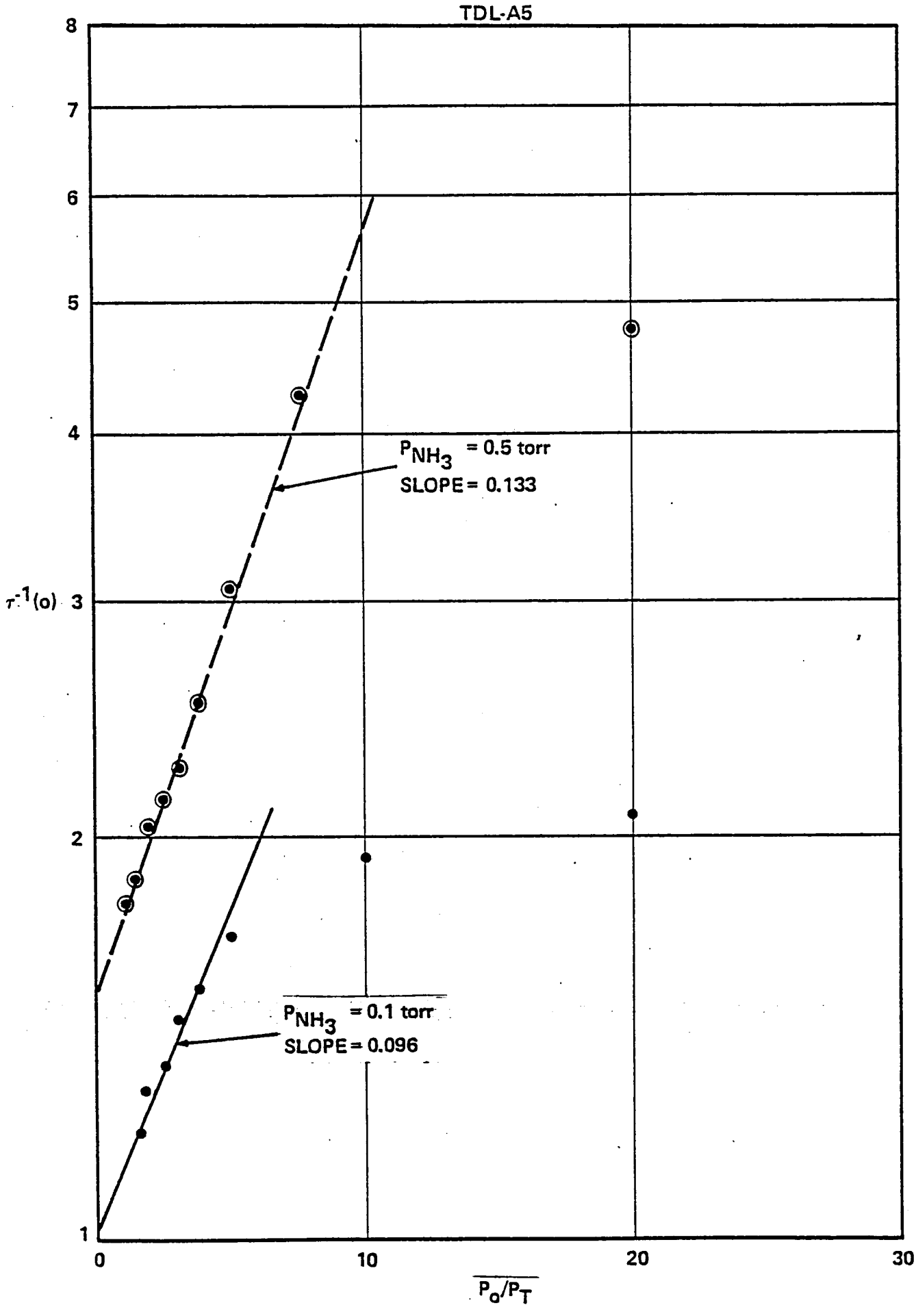

Figure 4-11. Measured Line-Center Transmission vs Total Cell Pressure Using Heterodyne Measurement Setup for T = 57.9 K and ν_o = 930.76 cm^{-1}

Page 4-27
Missing
From
Original

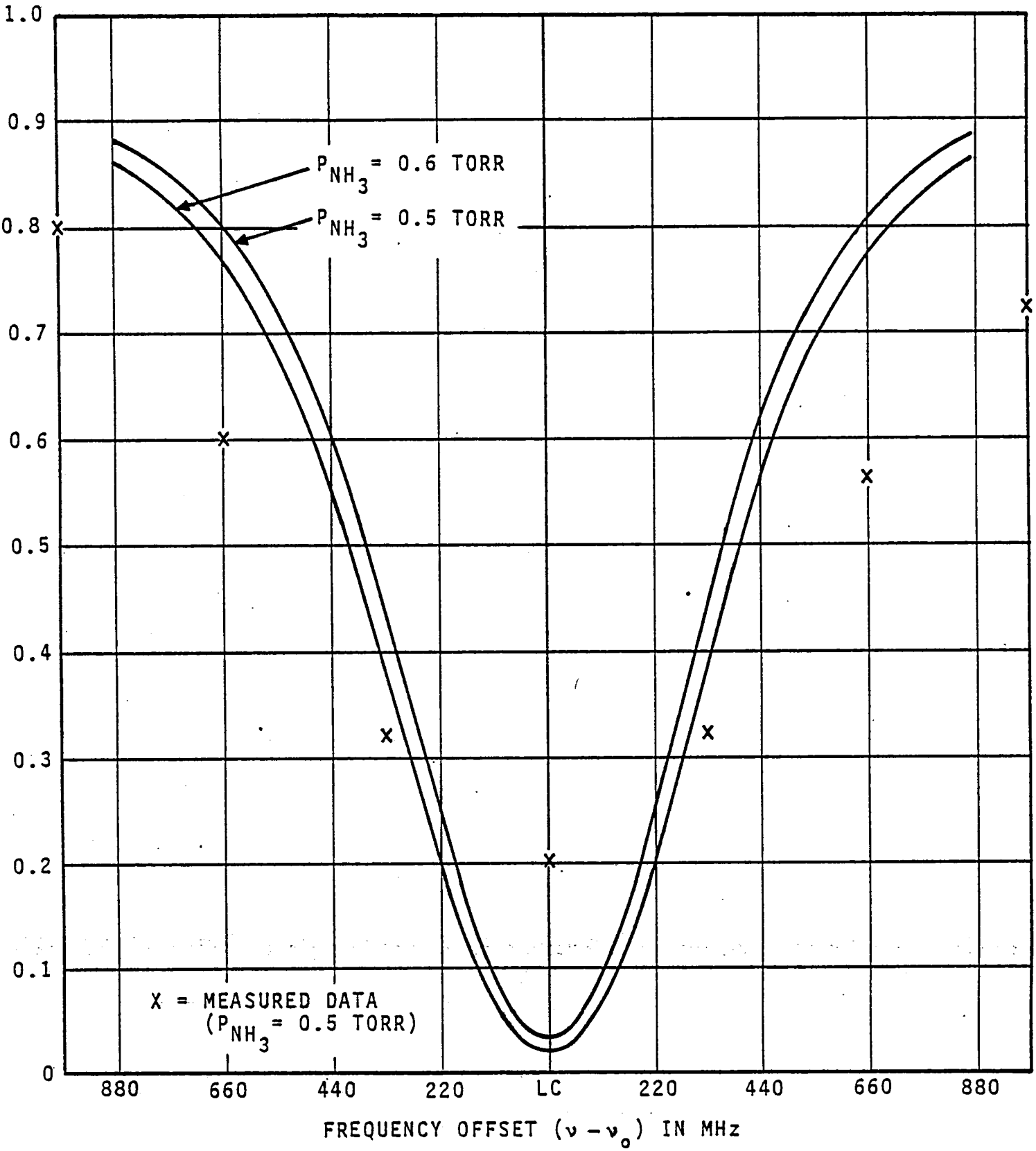

FIGURE 4-13. MEASURED AND CALCULATED AMMONIA ABSORPTION LINE SHAPES FOR A TOTAL PRESSURE OF 38 TORR, B = 150 MHz, ν_o = 930.76 cm^{-1}

Table 4-2. Heterodyne Spectroscopy: Measured and Calculated Ammonia Linewidths for $\nu_o = 930.76$ cm^{-1} and B = 150 MHz

P_T (torr)	Half Width at Half Maximum (MHz)		
	P_{NH_3} = 0.1 torr		P_{NH_3} = 0.2 torr
	Measured	Calculated	Calculated
38	~350	~242	~275
76	~610	~330	~375

As may be seen from the table, the measured linewidths are greater than the calculated linewidths in all cases.

Measured and calculated linewidths for P_{NH_3} = 0.5 torr are given in Table 4-3.

Table 4-3. Heterodyne Spectroscopy: Measured and Calculated Ammonia Linewidths for $\nu_o = 930.76$ cm^{-1} and B = 150 MHz

P_T (torr)	Half Width at Half Maximum (MHz)		
	P_{NH_3} = 0.5 torr		P_{NH_3} = 0.6 torr
	Measured	Calculated	Calculated
19	~610	~286	~320
38	~685	~396	~415
76	~735	~506	~550

Again, for all cases investigated, the measured ammonia spectral linewidth was greater than the calculated value. It may be noted that the

use of a somewhat higher NH_3 partial pressure for the linewidth calculations tends to increase the agreement between the measured and calculated data. The data in Table 4-3 also indicate that the agreement between the calculated and the measured linewidth values improves with increasing total pressure. This suggests that the discrepancy between the calculated and measured spectral linewidths may be the result of a larger effective receiver bandwidth than was previously assumed.

As in the case of the direct detection TDL spectroscopic measurements (Section III-E), the measured transmission through the wings of the selected ammonia line was considerably less than predicted. Several possible causes for this discrepancy are discussed below.

1) TDL Tuning Rate Uncertainty

Any error in the determination of the TDL tuning rate ($\Delta\nu/\Delta I$) will lead to a change of the frequency axis. The nominal tuning rate of 110 MHz/mA was determined from measurements taken over a wider range of TDL injection current than is required for the lineshape measurements. Other investigators have reported non-linearities over relatively small ranges of injection current (Ref. 4). While it is possible that such nonlinearity may have existed during the measurements, the likelihood of this factor being the sole explanation of the observed deviation is believed to be small.

2) Interference From Neighboring Spectral Lines

Another factor which may contribute to a lower value of transmission is the interference of neighboring absorption lines. In the particular region of the spectrum under consideration the strong spectral lines are approximately 0.4 cm^{-1} apart (Ref. 10). Such a spectral spacing between lines is wide enough so that a pair of lines would interfere only slightly with each other. However, since there are many more lines than just a single pair, their cumulative effect may be significant. (It can be noted at this point that measurements were performed using the test cell filled with various pressures of pure N_2. No absorption structure of any kind was observed during these measurements.)

3) Uncertainty of the Ammonia Self-Broadening Coefficient

Since the collision-broadened linewidth is dependent on the self-broadening coefficient B as noted in equation (A-9) of Appendix A, knowledge of B is required for an accurate calculation of the lineshape. In equation (A-9) it can be seen that if $P_{NH_3} = P_T$, then, at $P_{NH_3} = P_o$ and $T = T_o$, $\gamma_C = B\gamma_o$ resulting in the value of $\gamma_C = 0.599$ cm^{-1} atm^{-1} (given by Taylor, Reference A3). Also if $P_{NH_3} \ll P_T$ then, at $P_T = P_o$ and $T = T_o$, $\gamma_C \simeq \gamma_o$; resulting in the value of $\gamma_C = 0.08$ cm^{-1} atm^{-1} (given by Hinkley, Ref. A-4). B can then be determined to be of the order of 7.5. However at the selected values of P_{NH_3} the change due to this value of B in the calculated curves is not sufficient to account for any more than a minor part of the discrepancy between the measured and calculated lineshape data.

4) Measurement Limitations Related to Spectrometer Noise

The apparently better agreement between the calculated and measured transmissions for low NH_3 partial pressure (as shown in Figure 4-12) suggests a fourth possible explanation for the disagreement. If the transmission should decrease to a value below the minimum amount detectable by the spectrometer then it would be impossible for the experimental data to agree with the theoretical curves at every point. That this was not happening is clear from the fact that in every case the transmission at line center was greater than zero.

Since a radiometer determines relative power differences, the setting of a zero reference point is somewhat arbitrary. In the particular measurement setup used for the ammonia linewidth measurements, zero transmission was determined by filling the test cell with NH_3 and noting the spectrometer output voltage. One hundred percent transmission was measured by evacuating the test cell and noting the output voltage. The so-called zero level is, in reality, the noise level of the instrument or, equivalently, that voltage corresponding to the minimum detectable transmission.

Because the minimum transmission must always occur at line center an understanding of the behavior of line center as a function of pressure is necessary to more complete understanding of the spectrometer's output; from equation (A-3) (Ref. A1):

$$\frac{\beta(o)}{\beta_o} = e^{a^2}\left[1 - \text{erf}\,(a)\right] \qquad (4\text{-}5)$$

However, since it has already been determined that the Lorentz shape is appropriate for the pressure region in which the measurements were performed, from equation (A-10):

$$\beta_C(o) = \frac{N S_o}{\pi} \cdot \frac{1}{\gamma_C} \qquad (4\text{-}6)$$

Since γ_C is dependent upon pressure according to equation (A-9), then equation (4-6) may be rewritten as:

$$\beta_C(o) = \frac{N S_o}{\pi \gamma_o} \cdot \frac{P_o}{P_T} \qquad (4\text{-}7)$$

for the case in which B can be neglected and $T = T_o$. Using equations (A-2) and (4-7), the transmission at line center of a collision-broadened line is given by:

$$\tau(o) = \exp\left[- \frac{N S_o L}{\pi \gamma_o} \cdot \frac{P_o}{P_T} \right] \qquad (4\text{-}8)$$

Measured values of $\tau(o)$ for different values of N (or equivalently P_{NH_3}) were given in Figures 3-12 and 4-11. A computer was employed to calculate $\tau(o)$ for a heterodyne receiver with B = 150 MHz; its results are given in Figures 4-14 and 4-15. (Calculations for a receiver bandwidth of B = 100 MHz corresponding to a direct detection receiver were given in Figure 3-14.)

The divergence of the measured data from the calculated curves in Figures 4-14 and 4-15 may be caused by several factors. One of these is the variance of cell pressure which could have occurred during the repeated filling of the test cell. Such errors are the probable cause of the differing linear slopes and of some of the point scatter in Figures 3-14, 4-14, and 4-15.

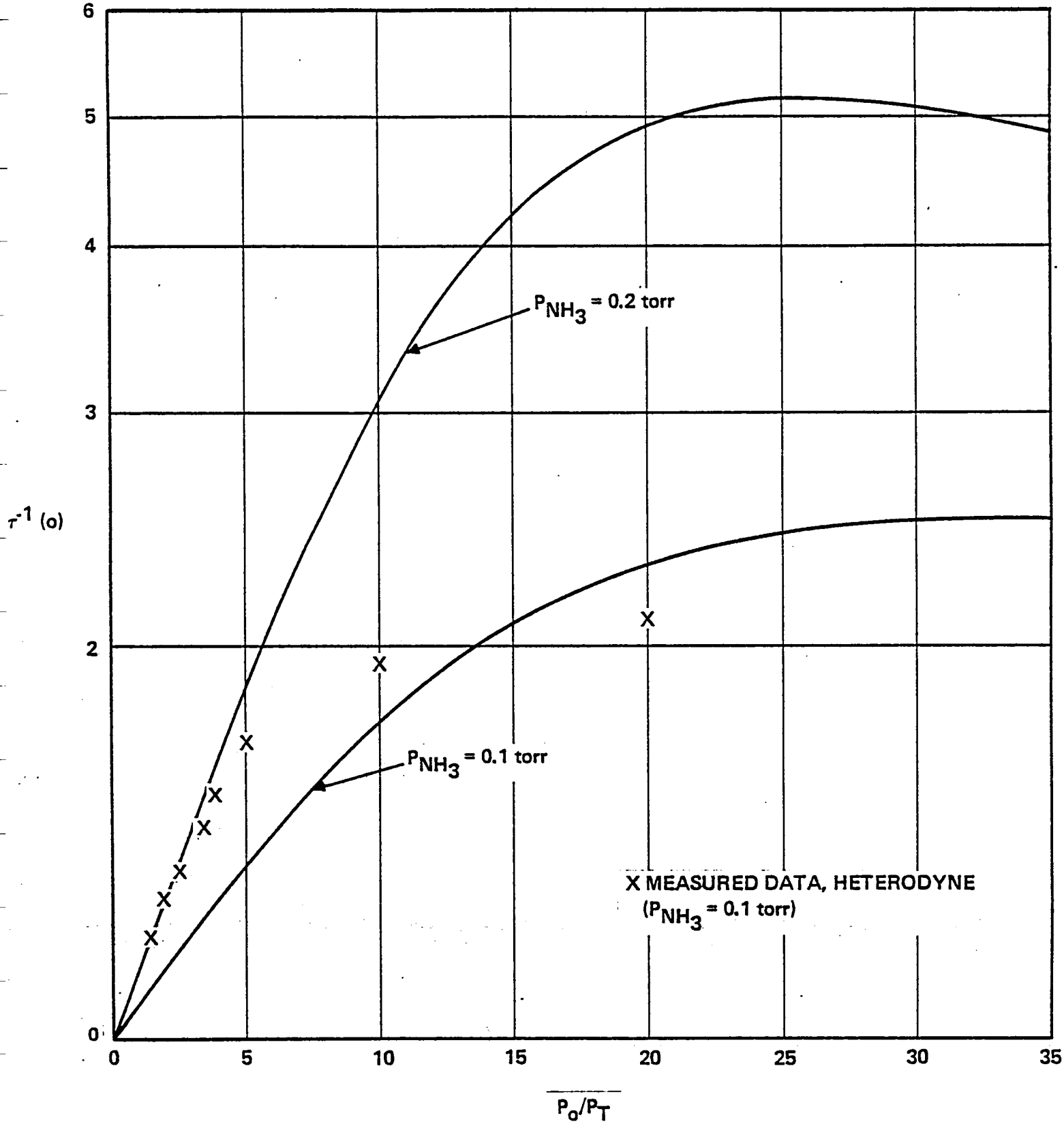

Figure 4-14. Measured and Calculated Line Center Transmission for P_{NH_3} = 0.1 torr and B = 150 MHz

$\overline{\nu_o}$ = 930.76 cm^{-1}

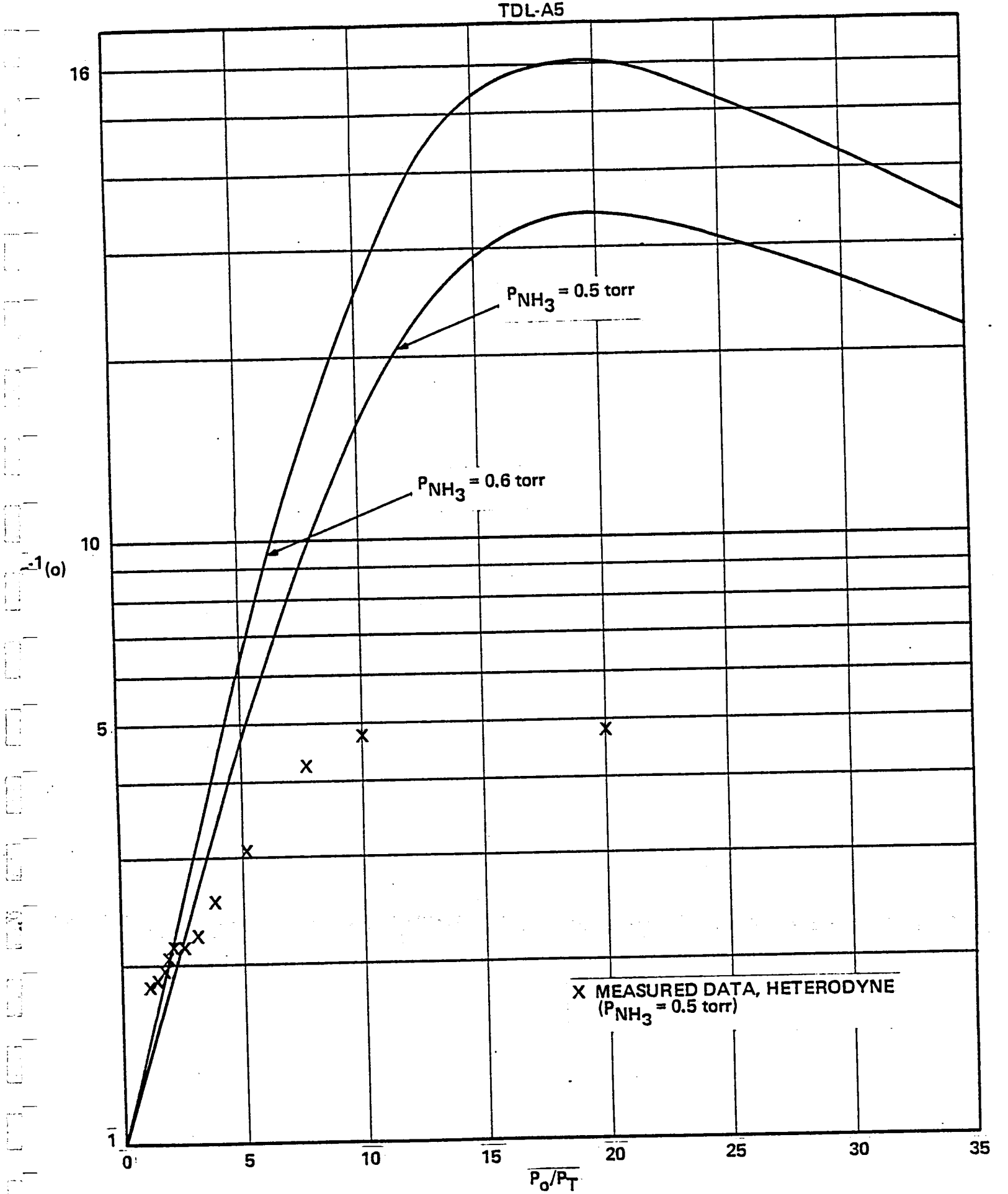

Figure 4-15. Measured and Calculated Line Center Transmission for P_{NH_3} = 0.5 torr and B = 150 MHz
ν_o = 930.76 cm^{-1}

5) Spectral Settability of the TDL Local Oscillator

Equation (4-8) is valid only at absorption line center; any frequency offset caused by a misadjustment of the diode laser LO can have a large effect on the measured transmission. At low pressures, corresponding to narrow spectral lines, the measurements are particularly sensitive to this effect. Figure 4-16 shows calculated curves of the inverse of the nominal line center transmission versus the inverse of P_T for several LO frequency offsets, a fixed NH_3 partial pressure, and a single-sided measurement bandwidth of 150 MHz. The actual experimental setup may have approximated these conditions. Figure 4-17 shows calculated curves for the same conditions except that the assumed measurement bandwidth was increased to 300 MHz. As might be expected the effect of a LO frequency offset on the measured transmission of a line whose width is comparable to the measurement bandwidth is greater than the effect of the same offset on a line whose width is smaller than the measurement bandwidth. While a frequency offset may have occurred during the measurements, it is apparent from the lineshapes (Figures 3-13, 4-12, and 4-13) that such an offset must have been less than $\pm$ 50 MHz (corresponding to an injection current variation of $\pm$ 0.45 mA). Since smooth curves can be drawn through the measured points, including the points assumed to be at line center, it is clear that the diode laser frequency was accurately and repeatably adjustable to line center.

6) Errors Due to TDL Bandwidth

Another possible explanation of the differences between the theoretical and experimentally measured ammonia lineshapes involves the effective receiver measurement bandwidth. As the measurement

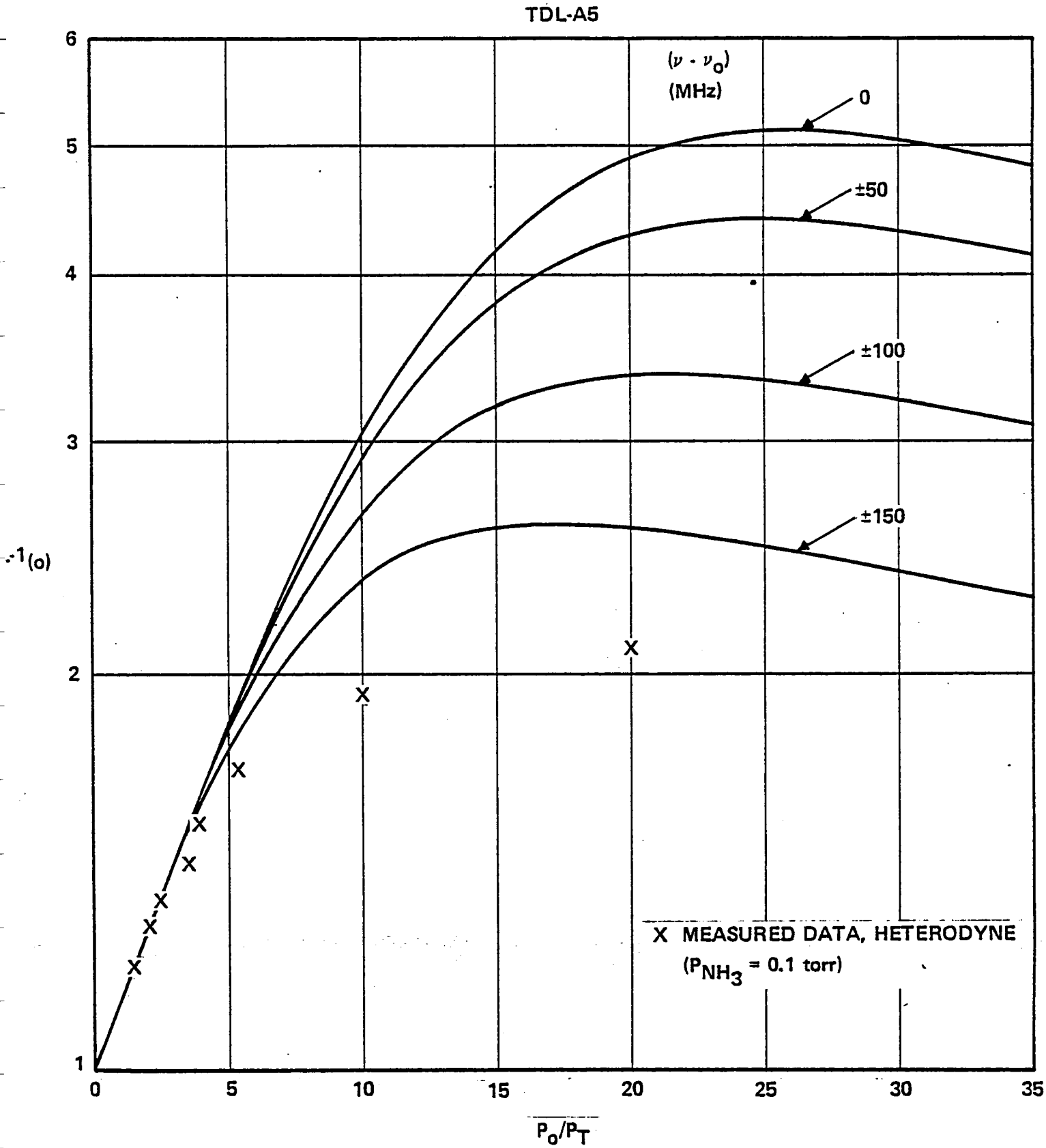

Figure 4-16. Calculated Line Center Transmission for P_{NH_3} = 0.2 torr and B = 150 MHz With LO Frequency Offset a Parameter

ν_o = 930.76 cm^{-1}

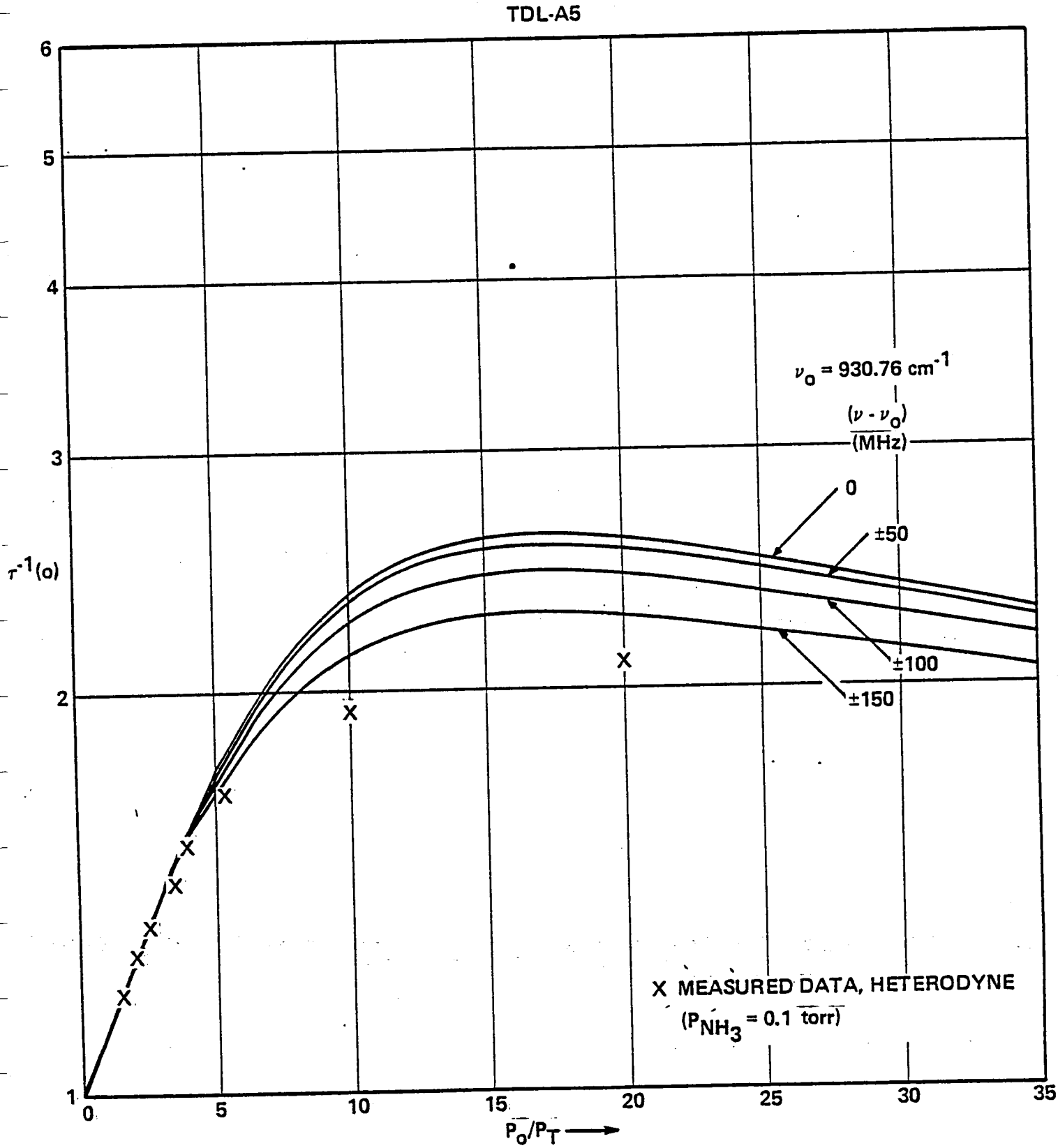

Figure 4-17. Calculated Line Center Transmission for P_{NH_3} = 0.2 torr and B = 300 MHz With LO Frequency Offset a Parameter

bandwidth increases the calculated ammonia lineshape becomes broader as indicated in Figure 4-18. Based on the curves in Figure 4-18, the actual measurement bandwidth appears to be approximately 400 MHz.

Since the integral of $\beta(\nu)$ is a constant, according to equation (A-11), the line center transmission must increase with increasing bandwidth as shown in Figures 4-18 and 4-19. The measured points in Figures 4-18 and 4-20 were obtained using the heterodyne spectrometer, while the measured points in Figure 4-19 were obtained using the direct detection measurement setup. The data in these figures indicate that the measurement bandwidths are larger than the previously assumed 150 MHz for the heterodyne setup, and 50 MHz for the direct detection setup.

The integration time of the backend processor of the heterodyne spectrometer was set at 30 seconds; this time constant required at least a two minute observation time per measured point. It is possible that the frequency deviation of the diode laser during the several minutes necessary for a spectroscopic measurement was larger than the value recorded during the few seconds required to make the frequency stability measurements described in Section 4-A. Since the bandwidth of the processor is accurately known to be 100 MHz, any increase in the effective instrument bandwidth required for theory-experiment agreement can be attributed to spectral instabilities in the diode laser.

From Figure 4-20, the effective instrument bandwidth can be estimated to have been between 300 MHz and 400 MHz. With a processor bandwidth of 100 MHz, the diode laser frequency deviation over several

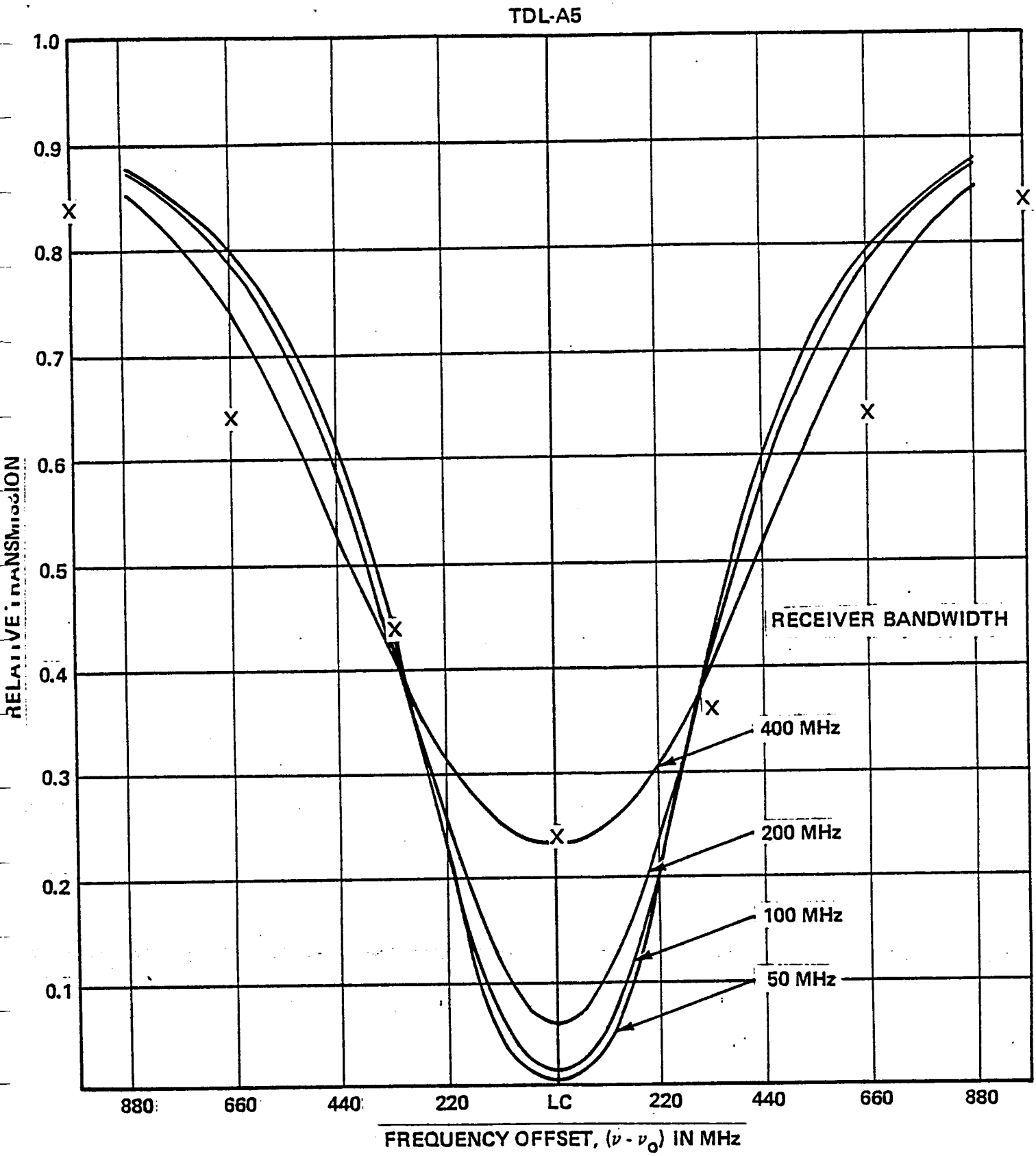

Figure 4-18. Measured and Calculated Ammonia Lineshapes for P_{NH_3} = 0.5 torr, P_T = 38 torr, and ν_0 = 930.76 cm^{-1} With Receiver Bandwidth a Parameter

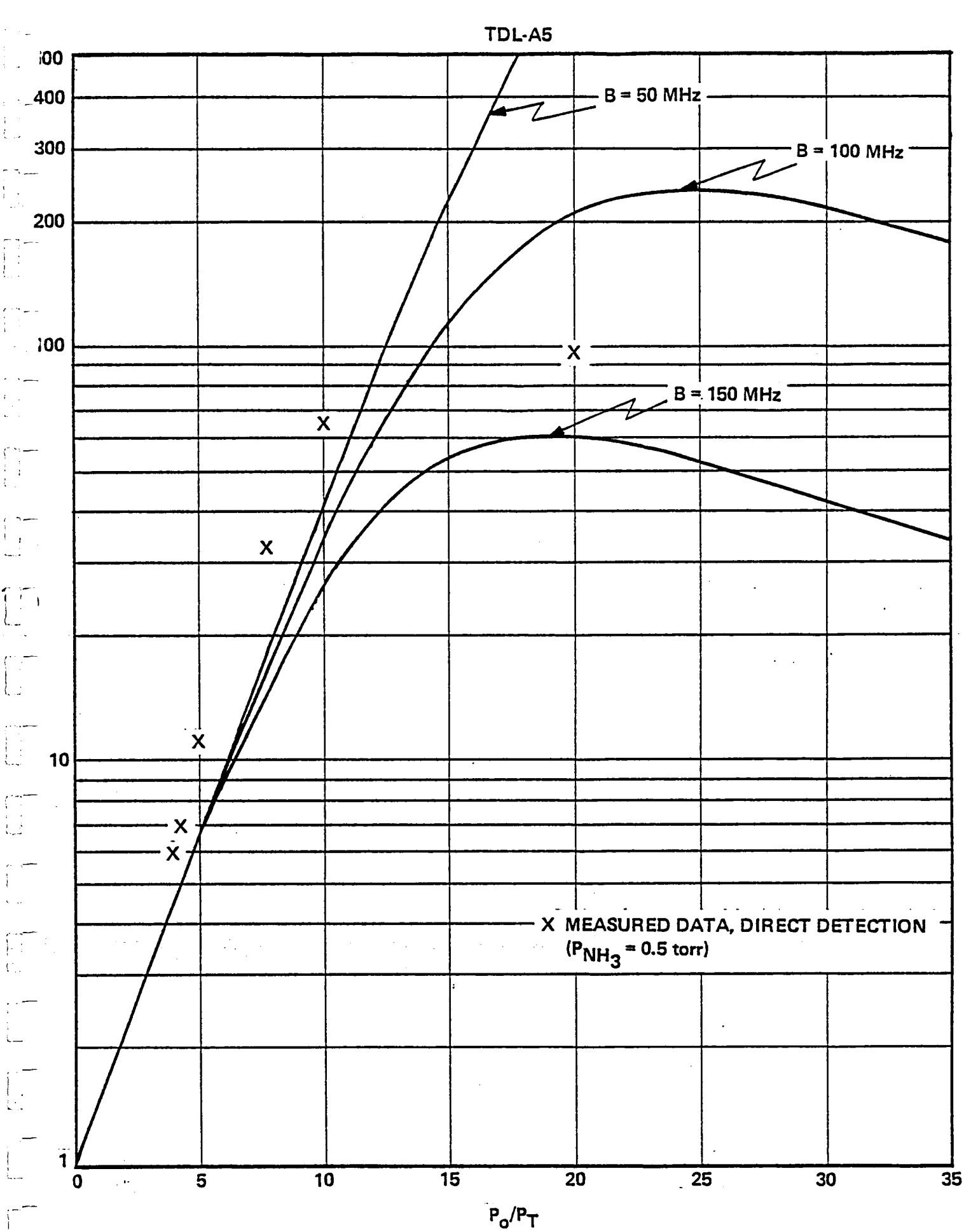

Figure 4-19. Calculated Line Center Transmission for P_{NH_3} = 0.6 torr and ν_o = 930.76 cm^{-1} With Receiver Bandwidth a Parameter

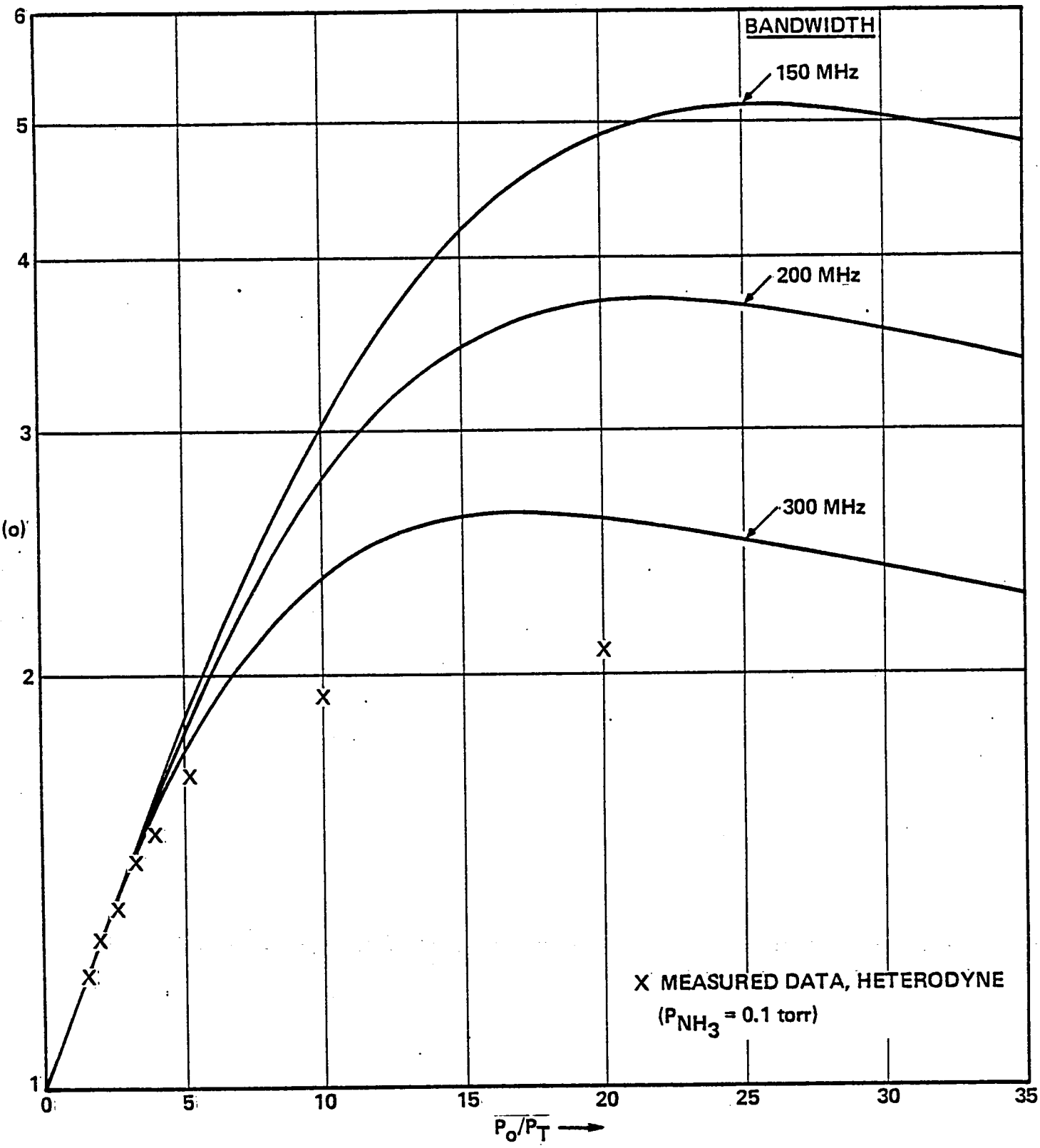

Figure 4-20. Calculated Line Center Transmission for P_{NH_3} = 0.2 torr and ν_o = 930.76 cm^{-1} With Receiver Bandwidth a Parameter

minutes can be inferred to be approximately ± 250 MHz. This is considerably larger than the frequency deviation of ± 45 MHz that was measured over one second. It may also be observed from Figure 4-19 that the TDL frequency deviation is only approximately ± 125 MHz. The data shown in this figure were obtained from the direct detection setup in which each measurement required only ten seconds. It might, therefore, be expected that the frequency deviation required in Figure 4-19 is less than that required in Figures 4-18 and 4-20.

As noted previously in Section 4-A, the frequency stability of the diode laser was corrupted by the mechanical vibrations induced in the device by the closed cycle refrigerator. These vibrations occur with a repetition frequency of 2-3 Hz which makes them fast phenomena which are integrated by the long time constant of the Dicke radiometer. Also, the heterodyne measurement time requirements allow the inclusion of possible longer term error components due to power supply and refrigerator temperature drift.

7) Calculation Errors

The final possible cause of the discrepancies between the calculated and the measured lineshapes may be contained in the calculations themselves. Small changes in the values of S_o and γ_o have profound effects on any subsequent calculations involving these parameters. The assumed Lorentzian lineshape may not be perfectly accurate at the pressures which were considered but the Voigt shape's steeper sides and greater line center absorption are exactly opposite to the observed line characteristics. One

correction to the calculations which does alter them toward the measured results involves the assumption that the test cell gas was optically thin. If this assumption is correct then the total power of a 1273K blackbody source transmitted through the test cell is given (equation A-2) by:

$$P_{TR} = P_{1273} \exp\ (-\beta(\nu)L) = P'_o \qquad (4\text{-}9)$$

where P_{TR} is the transmitted power, P_{1273} is the blackbody source power and P'_o is the observed power. (Over a reasonably small wavelength interval Planck's irradiance may be considered to be a constant.) If the gas is thick, however, some of the energy absorbed will be re-emitted by the gas with a spectral distribution determined by the average temperature of the gas. Since, in the experiment under consideration, the gas temperature was 300K, this re-emitted power can be written as:

$$P_R = P_{300}\ \epsilon(\nu) \qquad (4\text{-}10)$$

where $\epsilon(\nu)$ is the gas emissivity as a function of wavelength. The signal power available at the photomixer for heterodyne detection is the sum of these two terms:

$$P_0 = P_{TR} + P_{RE} \qquad (4\text{-}11)$$

The emissivity is related to the transmissivity by:

$$\epsilon(\nu) = 1 - \exp\left[-\beta(\nu)L\right] \qquad (4\text{-}12)$$

Combination of (4-9), (4-11), and (4-12) with the fact that $P_{300}/P_{1273} = 2.3 \times 10^{-2}$ at a wavelength of 10.78 micrometers gives:

$$\frac{P_0}{P'_0} = \frac{2.3 \times 10^{-2}}{\exp\left[-\beta(\nu)L\right]} + (1-2.3 \times 10^{-2}) \qquad (4\text{-}13)$$

which is the correction factor to the thin gas assumption.

From (4-13) it can be observed that the difference between a thin and thick gas is small for relative transmissions greater than about 10 percent. The following table lists the values of the correction factor, P_0/P_0', and the corrected transmission, P_0, for a few values of the uncorrected transmission, P_0'.

Table 4-4. Comparison of Transmissivities of Thin and Thick Gases

P_0' (percent)	$\frac{P_0}{P_0'}$	P_0 (percent)
100	1.0	100
50	1.023	51
10	1.210	12
5	1.443	7
1	3.277	3

It is clear from Table 4-4 that the corrected value of transmission are within the spectrometer error which was approximately five percent.

In conclusion, analysis of the spectroscopic measurement data indicates that the measurement of spectral lineshape appears to be limited by the spectral stability of the TDL sources. In particular, spectroscopic measurements which require the use of long integration times place stringent requirements on the stability of the TDL refrigerator and power supply. The data in this section suggest that the refrigerator system (and/or current driver) used for the reported ammonia measurements must be improved to permit accurate spectroscopic investigations.

V. SUMMARY AND RECOMMENDATIONS

Two tunable diode lasers (TDLs) have been experimentally evaluated to establish their suitability for use as local oscillators (LOs) in infrared heterodyne spectrometers. These state-of-the-art TDLs were evaluated in both direct-detection and heterodyne detection measurement modes. The data obtained have been analyzed to determine the potential uses of TDLs in high resolution spectrometry.

A dual channel infrared heterodyne radiometer (IHR) which includes two discretely tunable CO_2 gas lasers has been previously employed to carry out remote atmospheric profiling measurements of stratospheric ozone and tropospheric ammonia (References 15 and 20). The CO_2 laser emits discretely over portions of the 9 to 11 μm wavelength but does not spectrally coincide with all of the vibrational-rotational lines of the atmospheric species of interest.

Diode lasers formed of different alloys operate over a wavelength range of less than 1 μm to greater than 30 μm. They can be tailored to overlap spectral lines of interest by adjusting the stoichiometry of the semiconductor alloy and fine tuning the emission output by variation of the TDL temperature and injection current. The TDLs evaluated on this program were designed to overlap (1) an output transition of the CO_2 gas laser at $\nu' = 927.3\ cm^{-1}$, and (2) a region of numerous spectral absorption lines of gaseous ammonia.

The measured TDL tuning rates of $\Delta\nu/\Delta I \approx 110$ MHz/mA and $\Delta\nu/\Delta T \approx 16$ GHz per degree Kelvin fix the required stabilities of

the injection current supply and the TDL cooler. The single-mode TDL tuning range was approximately $\pm$ 0.5 cm^{-1} for modes near threshold and $\pm$ 0.3 cm^{-1} for modes at injection current levels above threshold. The measured spectral separation between laser modes was approximately 1.8 cm^{-1}. Based on the piecewise-continuous spectral tuning of the diode lasers, it is concluded that a TDL used in a heterodyne spectrometer must be carefully selected to insure the spectral overlap of an emission mode of the laser with an absorption line of interest. For multiple atmospheric species several TDLs may be required.

The output spatial intensity of a TDL generally exhibits a complex non-Gaussian distribution. Far-field TDL spatial pattern measurements as modified by a lens system (Fourier transform) have been carried out under single-mode and multi-mode TDL conditions. The measured single-mode intensity patterns exhibited a smooth, bell shaped pattern with half-power spatial widths of 25 μm x 28.5 μm. The 25 μm dimension agrees with the nominal TDL stripe width while the 28.5 μm dimension is believed to be related to the width of the TDL uniform current density region. The far-field spatial response is compatible with the laser LO requirements of a photomixer element of arbitrary geometry.

The maximum multi-mode TDL power levels measured were 200 μW at I_{DC} = 1.62 amperes for TDL-A5 and 175 μW at I_{DC} = 1.69 amperes for TDL-A6. The maximum single-mode power levels were 125 μW for TDL-A5 and 100 μW for TDL-A6. The output powers are available

in highly divergent beams which must be captured and collimated for heterodyne local oscillator applications. The single-mode TDL LO power available at the heterodyne photomixer was typically 20 to 80 μW. This power level is only a factor of three to ten below that required for efficient heterodyne spectrometer operation.

Measurements with a TDL and a high resolution Fabry-Perot Etalon (FPE) resulted in (a) spectral regions in which the single-mode output of the TDL did not significantly degrade the FPE's characteristics, and (b) spectral regions in which the TDL's multi-wavelength output greatly reduced the etalon's apparent finesse. A minor part of the reduced apparent finesse is attributable to imperfect collimation of the TDL's output while multi-wavelength emission accounts for the remainder. It is concluded that the multi-mode capability of TDLs imposes more restrictions on the use of these devices with FPEs than any collimation difficulties impose.

Heterodyne measurements using a multi-mode TDL local oscillator demonstrated that self-beating (double conversion mixing) effects degrade the overall heterodyne receiver sensitivity. IF spikes were observed in regions of triple wavelength output of a TDL. These measurements indicated that efficient heterodyne spectrometer operation will not be possible in spectral regions in which the TDL local oscillator exhibits a multi-wavelength output unless some mode selection element is incorporated into the TDL optical train.

Heterodyne receiver signal-to-noise ratio (SNR) measurements using a single-mode TDL local oscillator source resulted in a degradation factor of only 2.6 when compared to the measured SNR with a CO_2 gas laser LO. The measured and calculated heterodyne receiver SNRs exhibited excellent agreement for applied laser LO power levels between approximately 12 and 100 μW.

The short and long-term frequency stability of TDL-A5 was determined based on (a) two-laser heterodyne measurements, and (b) spectroscopic measurements of selected ammonia absorption line. Theoretically the emission "linewidth" of a semiconductor laser is less than 3 MHz, however effects such as TDL temperature and current instabilities and TDL vibrations cause spectral broadening of the laser's output. Using the two-laser heterodyne measurement setups the measured instantaneous (250 msec) frequency stability of TDL-A5 was approximately 30 MHz at the half-power points, while the frequency stability over a one-second time period was approximately 90 MHz. Frequency jitter caused by refrigerator operation was observed to be greater than 140 MHz over a two-second period.

Spectroscopic investigation of the aQ (3,3) spectral line in the Q branch of the ν_2 fundamental vibrational-rotational band of ammonia at $\nu_o = 930.76\ cm^{-1}$ resulted in measured spectral linewidths which were larger than calculated values in all cases. Using a direct detection measurement setup for $P_{NH_3} = 0.5$ torr and $P_T = 38$ torr, the measured half-width at half maximum (HWHM) linewidth, γ, was 585 MHz compared to a calculated value of 350 MHz, while at $P_{NH_3} = 0.5$ torr and $P_T = 76$ torr, the measured linewidth was

745 MHz compared to a calculated value of 468 MHz. Using the heterodyne spectroscopic measurement setup for P_{NH_3} = 0.5 and P_T = 76 torr, the measured HWHM linewidth was 735 MHz compared to a calculated value of 506 MHz. (It should be noted that the calculated spectral linewidths are different for the direct-detection and heterodyne-detection modes because of the differences in the receiver measurement bandwidth.)

A detailed analysis of possible causes for the discrepancies between the measured and calculated ammonia spectral linewidths was performed. This analysis suggests that ambiguity of the spectral stability of the TDL may be the principal cause of the discrepancy. In particular the long-term (greater than one second) frequency stability of the diode laser was corrupted by the mechanical vibrations in the TDL cooler and was inferred to be approximately 400 MHz.

Based on the TDL spectral linewidth and ammonia spectroscopic measurements carried out on this program, it is suggested that TDL frequency stability is the limiting factor in establishing TDLs as local oscillators for high resolution infrared heterodyne spectrometry. Although the instantaneous (250 msec) frequency stability of the TDL may approach 30 MHz, it should be noted that the remote monitoring of minor atmospheric species may require spectrometer integration times of 5 to 30 seconds, therefore, the long-term frequency stability of the TDL LO must be considered. Also, measurements of stratospheric species whose absorption linewidths approach the Doppler limit (typically less than 50 MHz HWHM)

will be more susceptible to TDL frequency stability effects than will measurements of tropospheric species whose linewidths may be collision-broadened to a few GHz.

The data in this report cover measurements of a single tunable diode laser (TDL-A5) over a five-month period. The TDL was temperature cycled between room temperature and 50K a total of six times during this test period with no severe degradation in TDL performance level.

Based on the laboratory measurements to date of the two TDLs, the prospects of using TDL local oscillators in heterodyne spectrometry are encouraging. Some further activities which are suggested include:

1) continue monitoring the characteristics of TDL-A5 to determine the long-term repeatability and resettability of the single-mode spectral regions as affected by time and temperature cycling;
2) improve the vibrational stability of the TDL cooler and repeat the long-term spectral stability measurements;
3) carry out laboratory measurements on additional TDLs;
4) repeat the heterodyne sensitivity measurements in an optimized test setup;
5) investigate the TDL frequency tuning rates for hysteresis effects;
6) investigate frequency mode separation and calibration techniques; and
7) investigate the variations of the TDL spatial patterns with temperature, current, and time.

REFERENCES

1. L.R. Tomasetta and C.G. Fonstad, IEEE J-QE QE-11, 384, (1975)
2. G.A. Antcliffe and J.S. Wrobel, Appl. Phys. Lett. 17, 290 (1970)
3. S.P. Chashchin, N.S. Baryshev, I.S. Averyanov, and N.P. Markina, Sov. Phys.-Semicond. 4, 989 (1970)
4. G.A. Antcliffe and S.G. Parker, J. Appl. Phys. 44, 4145 (1973)
5. G. Lasher and F. Stern, Phys. Rev. 133, A553 (1964)
6. J.C. Hill and G.P. Montgomery, Jr., Appl. Opt. 15, 748 (1976)
7. K.J. Linden, K.W. Nill, and J.F. Butler, IEEE J-QE QE-13, 720, (1977)
8. E.D. Hinkley and C. Freed, Phys. Rev. Lett. 23, 277 (1969)
9. J.F. Butler, A.K. Calawa, and T.C. Harman, Appl. Phys. Lett. 9, 427 (1966)
10. J.S. Garing, H.H. Nielsen, and K.N. Rao, J. Mol. Spect. 3, 496 (1959)
11. B.J. Peyton, A.J. DiNardo, G.M. Kanischak, F.R. Arams, R.A. Lange, and E.W. Sard, IEEE J-QE QE-8, 252 (1972)
12. B.J. Peyton, A.J. DiNardo, S.C. Cohen, J.H. McElroy, and R.J. Coates, IEEE J-QE QE-11, 569 (1975)
13. M. Mumma. T. Kostiuk, S. Cohen, D. Buhl, and P.C. von Thuna, Nature 253 (1975)
14. D.W. Peterson, M.A. Johnson, and A.L. Betz, Nature 250, 128 (1974)
15. B.J. Peyton, R.A. Lange, M.G. Savage, R.K. Seals, and F. Allario, AIAA Conference, Los Angeles, Ca. (1977)

REFERENCES (continued)

16. M.A. Frerking and D.J. Muehlner, Appl. Opt. 16, 526 (1977)

17. R.T. Ku and D.L. Spears, IEEE J-QE QE-13, 72D (1977)

18. D.E. Jennings and J.J. Hillman, NASA Publication X-693-77-143 (June 1977)

19. IBID, NASA Publication X-693-77-164 (July 1977)

20. B.J. Peyton, J. Hoell, R.A. Lange, R.K. Seals, Jr., M.G. Savage, and F. Allario, NASA Technical Memorandum NASA TM X-73630

APPENDIX A

THEORY OF SPECTRAL ABSORPTION LINES

This appendix presents expressions and data on the expected line strengths and line shapes for selected rotation-vibration spectral absorption lines. Constants appropriate to the consideration of ammonia are also presented.

The absorption of a length, L, of a gas is in general an exponential function which can be expressed via the Bouguer-Lambert law of absorption (Ref. A1) as:

$$\alpha(\nu) = \exp\left[\beta(\nu)L\right] \qquad \text{(A-1)}$$

where $\beta(\nu)$ is some function of pressure and wavelength. Equation (A-1) may be rewritten in terms of the transmission as:

$$\tau(\nu) = \exp\left[-\beta(\nu)L\right] \qquad \text{(A-2)}$$

The function $\beta(\nu)$, while explicitly dependent on ν, is also implicitly dependent on the partial pressure of the absorbing gas and on the total system pressure. The so-called Doppler region exists at very low values of pressure, i.e., below about 1 torr, and as the name implies is a regime in which the width of the absorption line, γ, is governed by the velocities of the individual absorbing molecules. The collision-broadened region occurs at pressures above about 70 torr and again as the name implies is a regime in which γ is governed by the elastic and inelastic collisions of the absorbing molecules and their environment. The pressure region between 1 torr and 70 torr is one of transition where neither Doppler broadening nor collision broadening is dominant.

The general expression of $\beta(\nu)$ for a single isolated absorption line is given (Ref. A1) by:

$$\frac{\beta(\nu)}{\beta_o} = \sqrt{\pi} \int_o^\infty \exp\left[-ax - \frac{x^2}{4}\right] (\cos \xi x)\, dx \qquad \text{(A-3)}$$

where:

$$\xi = \frac{\omega-\omega_o}{\omega_o} \left(\frac{mc^2}{2kT}\right)^{1/2} \qquad \text{(A-4)}$$

$$= \frac{\omega-\omega_o}{\gamma_D} (\ell n\ 2)^{1/2}$$

β_o is the limiting value of $\beta(\nu)$ at line center in the Doppler regime and is given by:

$$\beta_o = \frac{S_o}{\gamma_D} \sqrt{\frac{\ell n\ 2}{\pi}} \qquad \text{(A-5)}$$

γ_D is the half width at half maximum of the absorption line in the Doppler region. This linewidth is a function of not only the temperature and molecular weight of the absorbing particles but also of the absorption wavelength and is given by:

$$\gamma_D = (3.581 \times 10^{-7})\ \nu\ (T/M)^{1/2} \qquad \text{(A-6)}$$

The value of "a" in expression (A-3) is dependent upon the Doppler linewidth, γ_D, the collision-broadened linewidth, γ_C, and the so-called natural linewidth, γ_N, in the following way:

$$a = \sqrt{\ell n\ 2}\ \frac{\gamma_C + \gamma_N}{\gamma_D} \qquad \text{(A-7)}$$

but since γ_N is usually small compared to γ_C, (A-7) reduces to:

$$a \approx \sqrt{\ln 2}\ \frac{\gamma_C}{\gamma_D} \qquad (4\text{-}8)$$

The collision-broadened linewidth, γ_C, is dependent on the system's total pressure, P_T, and also on the partial pressure of the absorber which in this case is P_{NH_3}. The collision-broadened linewidth is given by:

$$\gamma_C = \frac{\gamma_o(P_T+(B-1)\ P_{NH_3})}{P_o}\sqrt{\frac{T_o}{T}} \qquad (A\text{-}9)$$

where γ_o is the value of the collisional linewidth as measured at some standard conditions of pressure (P_o) and temperature (T_o), and B is the self-broadening coefficient of the absorber. γ_C is also dependent to some extent on the particular gas used as a buffer.

Clearly the calculation of the $\beta(\nu)$ function (A-3) is not trivial; however, for small values of "a" (approximately 1) the expression reduces to the Doppler profile. As "a" increases beyond 3 or 4 the expression reduces to one first proposed by Lorentz which is given by:

$$\beta_c(\nu) = \frac{N\ S_o\ \gamma_C}{\pi(\gamma_C^2+(\nu-\nu_o)^2)} \qquad (A\text{-}10)$$

where N is the number of absorbing molecules per unit volume, ν_o is the line center frequency and S_o is the line strength given by:

$$S = \int_{-\infty}^{\infty} \beta(\nu)\ d\nu \qquad (A\text{-}11)$$

evaluated at the standard conditions P_o and T_o. For the temperatures and pressures which prevailed during the laboratory measurements, γ_D for the NH_3 absorption line at 930.758 cm^{-1} is readily determined using (A-6) to be 1.68×10^{-3} cm^{-1}.

Several investigators have determined the values of S and γ_o by both theoretical and empirical methods (Refs. A2, A3, A4). Taylor has taken these numbers to be 5.06×10^{-19} $cm^{-1}/mol\text{-}cm^{-2}$ and 0.599 cm^{-1} atm^{-1} respectively. However this value of γ_o is based on a pure NH_3 atmosphere. Because of the dependence of linewidth on the particular buffer gas used, γ_o will be taken to be 0.08 cm^{-1} in this report (Ref. A4). With these values of S_o and γ_o it is clear from (A-8) and A-9) that the Lorentz approximation is valid for the pressures under consideration.

APPENDIX REFERENCES

A1. S. Penner, "Quantitative Molecular Spectroscopy and Gas Emissivities," Addison-Wesley, 1959

A2. F. Allario, and R.K. Seals, Jr., Appl. Opt., 14, 2229 (1975)

A3. F.W. Taylor, J. Quant. Spectr. and Rad. Transf. 13, 1181 (1973)

A4. E.D. Hinkley, Report to the EPA, Contract F19628-70-C-0230 (1971)